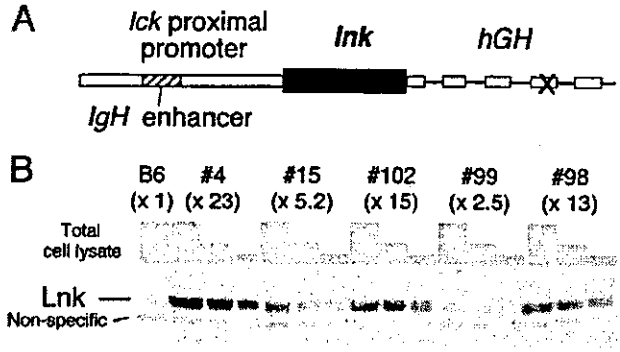

FIGURE 1. *A*, The p1026x-*lnk* transgene construct. The full-length cDNA fragment encoding the Lnk protein was inserted downstream of the *lck* proximal promoter and the Eμ enhancer, followed by the *hGH* mini gene cassette. The *hGH* gene carries a mutation in the fourth exon (indicated by an "X") so a functional hGH protein is not expressed. *B*, Lnk protein expression in thymocytes obtained from five independent transgenic mouse lines (Lnk numbers 4, 15, 102, 99, and 98) and control C57BL/6 (B6) mice. Serial dilutions (2-fold) of total cell lysates were separated by SDS-PAGE, and subjected to immunoblotting using anti-Lnk Abs. Lnk expression levels were determined by densitometry, and the fold expression over endogenous Lnk protein levels in nontransgenic C57BL/6 animals is indicated in parentheses under the transgenic line name. Amounts of lysates loaded in each lane can be estimated from nonspecific bands cross-reacted with our anti-Lnk Abs.

$B220^+$ cells, many of which were $CD43^+$ pro-B cells. Most of the pro-B cells were HSA^- and $BP\text{-}1^-$ (Hardy et al.'s fraction A; Ref. 1), indicating that B cell development was blocked at a very early stage. Other transgenic lines showed mild reduction of B lineage cells that correlated in a dose-dependent manner with the Lnk expression level (Fig. 3). Interestingly, the correlation between reduction of B lineage cells and Lnk expression levels was not a linear correlation. Instead, the reduction correlated with the logarithmic value of Lnk expression levels. The reduction of pre-B and immature B cells was more severe than that of pro-B cells. This may suggest the existence of Lnk-dependent regulation in the transition from pro-B to pre-B cell stages, in addition to the known role for Lnk in pro-B cell expansion (16). However, our pro-B cell discrimination based on the method of Hardy and colleagues (24) contains non-B lineage cells, especially in Fraction A ($B220^+$ $CD43^+HSA^-BP\text{-}1^-$). Thus, an alternative possibility could be that those non-B lineage cells in the pro-B cell fraction not expressing the transgene were maintained at relatively normal levels, leading to an underestimation of the pro-B cell reduction. As expected, no cell number reduction was observed in myeloid cells, which should not express the transgenes.

Impaired expansion of T precursors by Lnk overexpression

We next examined consequences of Lnk overexpression in T lineage cell development. Total thymocyte numbers declined as Lnk expression in thymocytes increased (Fig. 3). However, thymocyte development, evaluated on the basis of CD4 and CD8 expression, was grossly normal (Fig. 2), except for a slight reduction of $CD4^+CD8^-$ and $CD4^-CD8^+$ mature thymocytes. The reduction in number was slightly more severe in $CD4^-CD8^+$ thymocytes than that of $CD4^+CD8^-$ mature thymocytes in Lnk transgenic lines. Within the $CD4^-CD8^-$ immature thymocyte compartment, a proportion of $CD44^-CD25^+$ or $CD44^-CD25^-$ cells was significantly reduced in transgenic mice compared with normal littermates (Fig. 2). This led to the overrepresentation of $CD44^+CD25^+$ cells indicating inefficient transition of $CD44^+CD25^+$ to $CD44^-CD25^+$ cells or impaired expansion of $CD44^-CD25^+$ cells.

Consequence of Lnk overexpression in peripheral lymphocytes

The total cell number in the spleen was also reduced as more Lnk transgenes were expressed. Only a residual number of B cells remained in the spleen of the highest expresser, Lnk no. 4 (Fig. 2). T cell numbers also declined as Lnk expression increased, although B cell reduction was more prominent than that of T cells (Fig. 3). We then examined splenic B cell subfractions by staining for CD21, CD23, and IgM. This analysis demonstrated that the $CD21^+CD23^-IgM^{high}$ MZ B cells were relatively maintained in

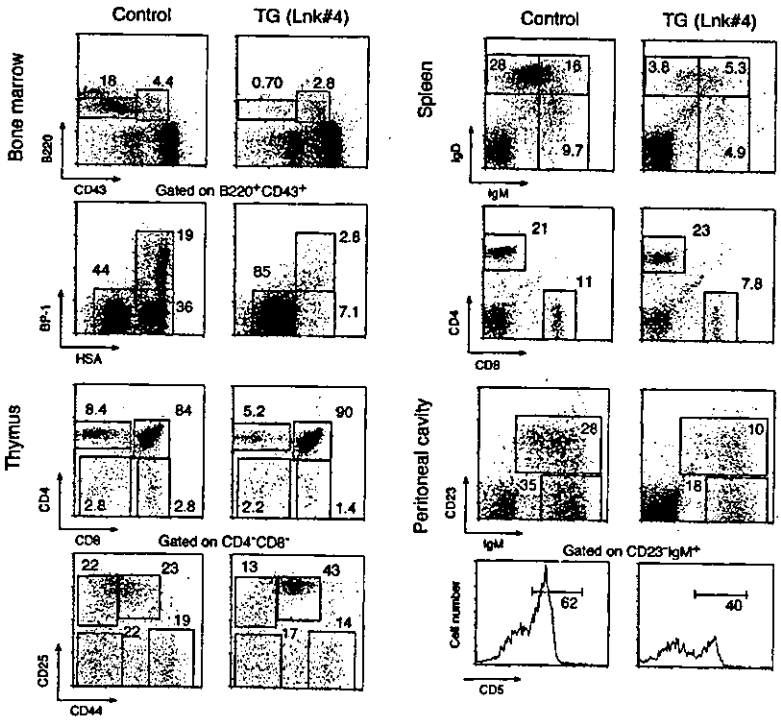

FIGURE 2. Representative multicolor fluorescence plots showing severe impairment of B cell development and mild reduction of T lineage cells in transgenic mice highly expressing Lnk protein (Lnk no. 4). Cell suspensions prepared from 6- to 8-wk-old animals were stained with combinations of labeled Abs and analyzed by flow cytometry. BM: expression of B220/CD45R and CD43 on total BM cells, and expression of BP1/Ly-51 and HSA/CD24 on $B220^+CD43^+$ pro-B cells. Spleen: total splenocytes were stained for surface IgM and IgD, or for CD4 and CD8. Thymus: expression of CD4 and CD8 on total thymocytes, and expression of CD25 and CD44 on $CD4^-CD8^-$ double-negative thymocytes. Peritoneal cavity cells: expression of IgM and CD23 on lymphocytes in peritoneal cavity, and expression of CD5 on $CD23^-IgM^+$ B1 cells. Numbers represent the percentages of cells in each box or area.

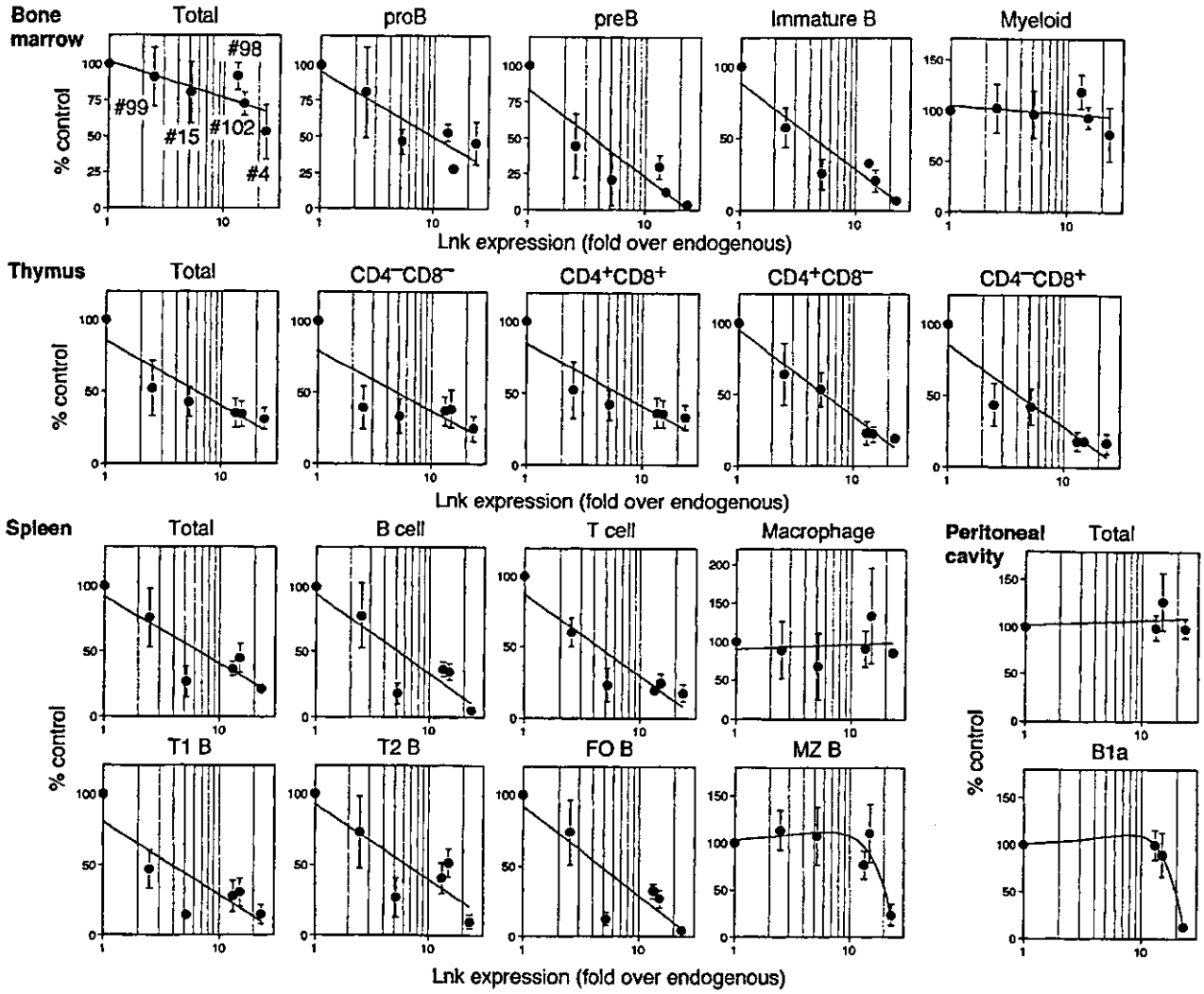

FIGURE 3. Dose-dependent reduction of lymphoid cells in p1026x-*lnk* transgenic mice. Cell suspensions prepared from 6- to 8-wk-old animals were analyzed by flow cytometry; the absolute cell numbers within each cell fraction were calculated and shown as percentage of those in littermate control mice. The relative amount of Lnk protein expressed in thymocytes from each transgenic line was assessed by immunoblotting and densitometry. Shown are means ± SD for four to six animals of each transgenic line. BM: pro-B ($B220^+CD43^+$), pre-B ($B220^+CD43^-IgM^-$), immature B ($B220^{low}IgM^+$), and myeloid cells ($B220^-CD43^+$). Spleen: B ($B220^+$), T ($CD3^+$), macrophages ($Mac\text{-}1^+$), transitional T1 B ($IgM^+CD23^-CD21^-$), transitional T2 B ($IgM^{high}CD23^+CD21^{high}$), FO B ($IgM^+CD23^+CD21^{low}$), and MZ B ($IgM^+CD23^-CD21^{high}$). Thymus: $CD4^-CD8^-$, $CD4^+CD8^+$, $CD4^+CD8^-$, and $CD4^-CD8^+$. Peritoneal cavity cells: B1a ($IgM^+CD23^-CD5^+$). B1 cells in the peritoneal cavity and MZ B cells are relatively resistant to Lnk overexpression.

most transgenic lines, except in the most potent expresser, Lnk no. 4. In contrast, all other peripheral B cell fractions in spleen, transitional T1 and T2 cells, and FO B cells decreased in a dose-dependent manner (Fig. 3). $CD23^-IgM^{high}CD5^+$ B1a and $CD23^-IgM^{high}CD5^-$ B1b cells in the peritoneal cavity were also relatively maintained in most transgenic lines, except in Lnk no. 4, whereas B2 cells and T cells in the cavity were reduced (Fig. 3 and data not shown).

Next, we examined whether Lnk overexpression affects the function of peripheral mature B cells. Lnk no. 98 moderately expresses Lnk protein (13-fold greater expression than endogenous Lnk in thymocytes) and was able to produce substantial numbers of splenic lymphocytes (~40% of normal C57BL/6 control mice). Histological and immunohistochemical analysis demonstrated that splenic architecture was grossly maintained in these transgenic mice, although the white pulp regions were reduced (data not shown). However, $CD21^+CD23^-IgM^{high}$ MZ B cells occupied a major compartment of splenic B cell populations (Fig. 4*A*). CD23 expression levels on $CD23^+IgM^{low}$ FO B cells in transgenic mice were slightly higher than those observed on normal FO B cells. $CD21^-CD23^-IgM^+$ T1 B cells showed slightly decreased IgM levels. In addition, T1, as well as $CD21^{high}CD23^+IgM^{high}$ T2, cells in transgenic mice were larger in size. In contrast, cells from other B lineage fractions, pro-B and pre-B cells, immature B cells in the BM, and FO and MZ B cells in the spleen were all similar in size to those of normal C57BL/6 mice (Fig. 4*B*). Interestingly, larger transgenic T1 cells were not actively proliferating (Fig. 4*C*). The cycling fraction of T1 B cells was severely reduced as assessed via DNA content analysis. In addition, expression levels of B cell activation markers, such as MHC class II and CD86 or CD25, on T1 cells were unchanged (data not shown). Thus, Lnk overexpression in peripheral splenic B cells compromised B cell maturation and proliferation, especially in the T1 fraction.

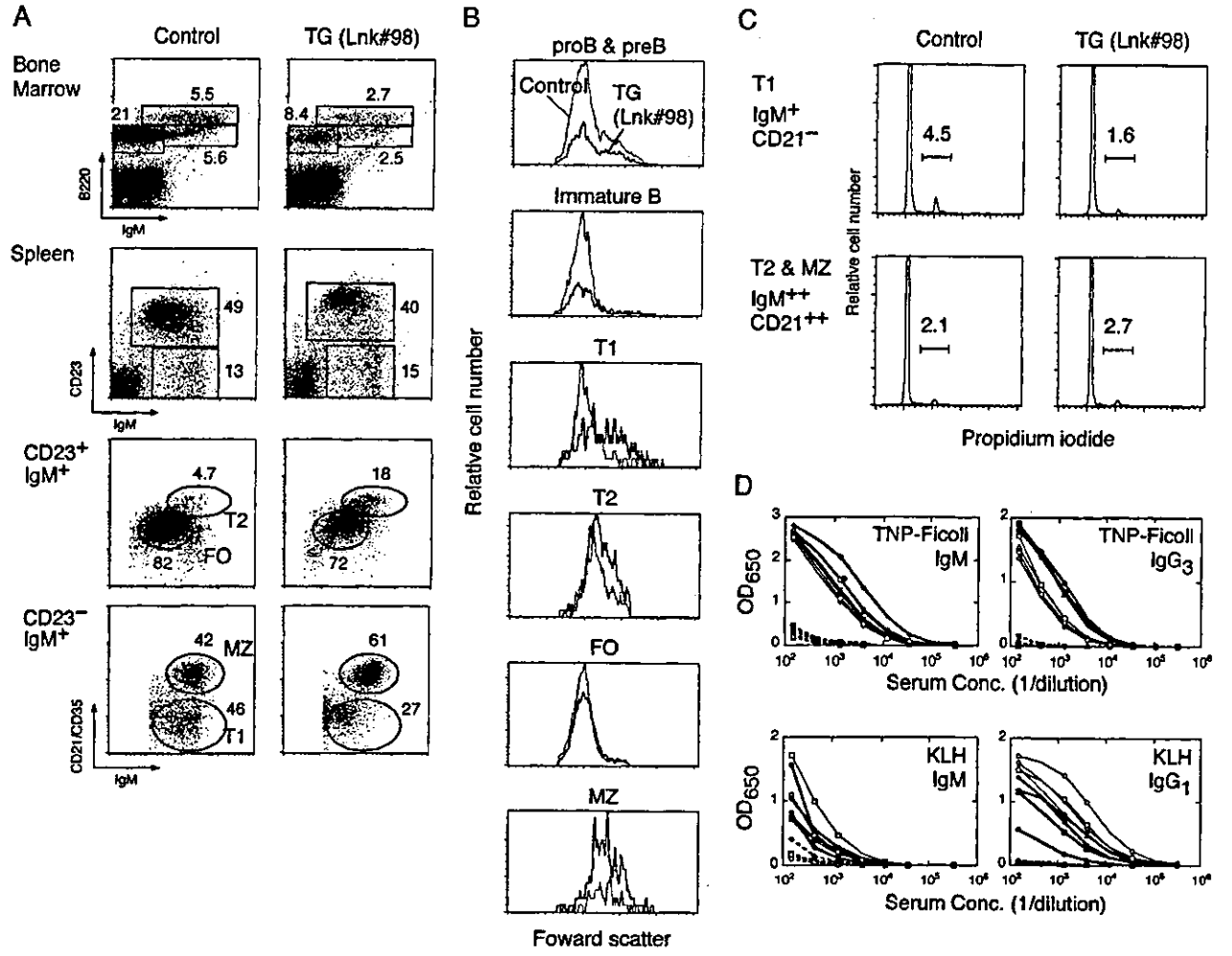

FIGURE 4. *A*, Representative multicolor fluorescence plots showing skewed splenic B cell compartments and increased cell size of transitional B cells in transgenic mice overexpressing Lnk at a moderate level (Lnk no. 98). BM: expression of B220 and IgM on total BM cells. Spleen: expression of CD23 and IgM on total splenocytes, and expression of CD21/CD35 and IgM on $CD23^+$ or $CD23^-$ splenic B cells. Numbers represent the percentages of cells in each box or area. *B*, Enlarged cell size of transitional T1 and T2 B cells in transgenic mice. Splenic B cells were fractionated electrically based on expression of IgM, CD23, and CD21/CD35. Forward scatter of transitional T1 B ($IgM^+CD23^-CD21^-$), transitional T2 B ($IgM^{high}CD23^+CD21^{high}$), FO B ($IgM^+CD23^+CD21^{low}$), and MZ B ($IgM^+CD23^-CD21^{high}$) were compared between control C57BL/6 (thin lines) and Lnk no. 98 mice (bold lines). *C*, Decreased cycling B cells in transgenic mice. T1 ($CD21^-IgM^+$), or T2 and MZ ($CD21^{high}IgM^+$) B cells were purified by cell sorting, fixed, and stained with propidium iodide. Numbers represent the percentages of cycling cells that fall into the indicated range. *D*, Response to TI-2 Ag, TNP-Ficoll (*upper panels*) and TD Ag, KLH (*lower panels*). Serial dilutions of serum obtained before immunization (dashed lines) or after immunization (solid lines) from control C57BL/6 mice (thin lines, open symbols) or Lnk no. 98 transgenic mice (bold lines, filled symbols) were analyzed for TNP- or KLH-specific Ig isotypes by ELISA.

Despite the reduced proliferation in the B cell compartment, in vitro proliferative responses of splenic B cells upon anti-IgM stimulation were only slightly impaired (data not shown). Ab production was also relatively well-maintained in *lnk*-transgenic mice. Reflecting the increased proportion of MZ B cells in the spleen and B1 cells in the peritoneal cavity, Ab production against a TI-2 Ag (TNP-Ficoll) was augmented in the *lnk*-transgenic mice compared with normal littermates. Sera of transgenic mice immunized with TNP-Ficoll contained a higher titer of anti-TNP Abs in both IgM and IgG3 subclasses (Fig. 4*D*). In contrast, IgM and IgG1 production against the TD Ag KLH was slightly compromised, which was consistent with the significant reduction of FO B cells in the spleen, and of T cells in the thymus and spleen. Interestingly, serum Ig levels of all subclasses were slightly increased in *lnk*-transgenic mice (data not shown). It seems that a strong signal through the B cell receptor could override the cell proliferation inhibition imposed by augmented expression of Lnk.

Negative regulation of lymphocyte development by Lnk is independent of its phosphorylation

Lnk contains a tyrosine phosphorylation motif involving Y536 at its C terminus that is conserved among all Lnk family adaptor proteins, including APS, SH2-B, and the Lnk-like protein in *Drosophila*. Y536 is the major site phosphorylated by c-Kit (20) and by various tyrosine kinases when simultaneously overexpressed in COS7 cells (S. Takaki, unpublished observation). We examined a potential role for the conserved tyrosine phosphorylation motif in the negative regulatory functions of Lnk in lymphocyte development. Y536 was substituted with a phenylalanine residue and the resulting mutant form of Lnk (Y536F) was inserted downstream of the *lck* proximal promoter and the Eμ enhancer, and expressed in lymphoid cells in transgenic mice. The Y536F transgenic mice expressed comparable amounts of Lnk protein with the mice expressing the wild-type Lnk. Lnk no. 4 (Fig. 5*B*). As in the case of

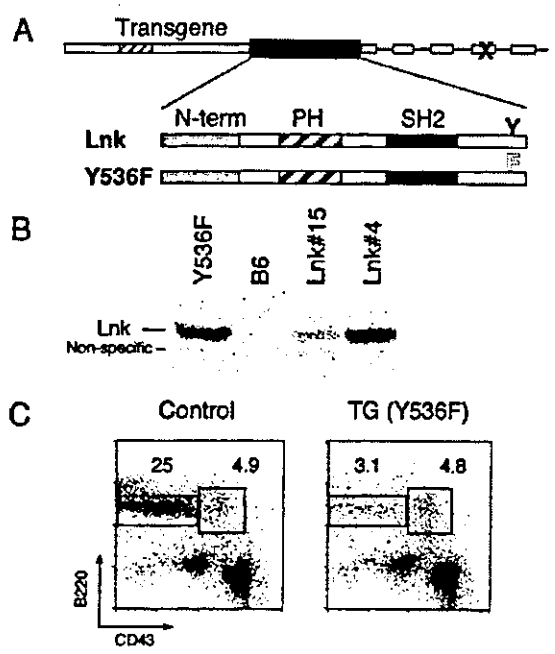

FIGURE 5. *A*, The transgene construct for the expression of Y536F mutant Lnk. The cDNA fragment encoding Lnk protein carrying a substitutional mutation of phenylalanine for tyrosine at position 536 (Y536F) was inserted downstream of the *lck* proximal promoter and the Eμ enhancer. *B*, Amounts of mutant Lnk protein in thymocytes obtained from Y536F transgenic mice were compared with those of Lnk protein in thymocytes from Lnk nos. 4, 15, and C57BL/6 (B6) mice. Equal amounts of total cell lysates were separated by SDS-PAGE, and subjected to immunoblotting using anti-Lnk Abs. *C*, Impairment of conventional B cell development in Y536F transgenic mice. Representative multicolor fluorescence plots showing expression of B220/CD45R and CD43 on total BM cells. Numbers represent the percentages of cells in each box.

wild-type Lnk overexpression, B cell development in Y536F transgenic mice was also inhibited at the pro-B cell stage. The BM contained very few $B220^+$ cells, which were mostly $CD43^+$ pro-B cells, similar to the BM of Lnk no. 4 transgenic mice (Figs. 5 and 1). The numbers of thymocytes and B1 cells in the peritoneal cavity were also decreased in the Y536F transgenic mice (data not shown). These results indicate that the Lnk C-terminal tyrosine phosphorylation site is dispensable for the negative regulatory effects of overexpressed Lnk in lymphocyte development.

Discussion

Lnk constrains lymphocyte production

Our results document a potent regulatory mechanism in lymphopoiesis mediated by the adaptor protein, Lnk. Lnk overexpression in lymphoid precursors resulted in both B and T cell reduction. Expansion of pro-B cells in bone marrow, and of pro-T cells in thymus was impaired as Lnk expression increased. We previously reported that mutant mice lacking the *lnk* gene showed enhanced B cell production due to the hypersensitivity of B cell precursors to SCF, a c-Kit ligand. However, the $lnk^{-/-}$ mice do not show any abnormality in T cell development or altered thymocyte expansion as seen in *lnk*-transgenic mice (16). B lineage cells express more Lnk than T lineage cells (15). Thus, different levels of endogenous Lnk expression in B lineage cells from those found in T lineage cells probably account for this discrepancy. In other words, Lnk could function in both B and T precursor cells, however, B precursors that express higher amounts of Lnk are more stringently controlled by Lnk-mediated regulatory signals. The physiological importance of this more stringent restriction of conventional B cell production by Lnk remains to be elucidated. In the C57BL/6 background, loss of the *lnk* gene alone does not cause autoimmunity, malignant transformation of B lineage cells, nor exhaustive loss of hemopoietic progenitor cells. Although it is possible that other Lnk family proteins might compensate for some Lnk function in *lnk*-deficient T cells, T lineage cells do not express APS (25). Moreover, despite the homology between Lnk and SH2-B, many studies have demonstrated positive effects of SH2-B on cell growth and differentiation (26–32), while Lnk functions as a negative regulator of lymphopoiesis as clearly shown in this study and in the analysis of the *lnk*-deficient mice. We recently reported that male and female gonad maturation is impaired in $SH2\text{-}B^{-/-}$ mice, while both B and T cell development are normal (33). Thus, in $lnk^{-/-}$ T lineage cells, compensation by other Lnk-family members does not appear likely. The generation of *lnk, SH2-B* double-deficient mice will help to elucidate the special regulatory characteristics of thymic progenitors.

Both B and T cell numbers were reduced as the amount of Lnk exponentially increased. This contrasts with that of the perturbed lymphocyte development by the increasing activity of many effector enzymes, such as $p56^{lck}$, by overexpression (34) or by the decreasing activity of $p56^{lck}$, Erk1, and *ras* by their dominant negative mutants (21, 35, 36). All these examples show a linear correlation between phenotype and protein expression levels. SH2-B forms a pentameric complex through homotypic association via its N-terminal domain (30). Because the N-terminal domains of Lnk-family adaptors are conserved, Lnk may also manifest its function as a multimeric complex. In transfected COS7 cells, Lnk indeed exists as a multimer (S. M. Kwon and S. Takaki, unpublished observation). Lnk multimerization could account for the semilogarithmic relation between lymphocyte reduction and Lnk expression levels. The stoichiometries between Lnk complexes, membrane receptors, and signaling molecules may also contribute to this unique correlation between phenotype and Lnk expression levels.

Lnk function in peripheral lymphocytes

Many unrelated transgenic and gene-targeted models show an enlarged splenic MZ compartment (3). In several cases, the enlarged MZ phenotype is linked to compromised peripheral B cell generation. For example, $IL\text{-}7^{-/-}$ (37) and conditional *Rag*-knockout mice (38) show reduced B lymphopoiesis at precursor levels and develop a larger MZ B subset. The peripheral B cells in these mice with impaired B lymphopoiesis show an activated phenotype: increased expression of CD25, class II, and CD86, and augmented entrance into the cell cycle (37, 38). These properties could result from compensatory mechanisms which allow enhanced generation of the mature B cell compartment. The peripheral phenotype observed in our *lnk*-transgenic mice was similar to that observed in $IL\text{-}7^{-/-}$ or conditional *Rag*-knockout mice in terms of increased MZ B cells accompanied by reduced B lymphopoiesis, but not fully consistent with the phenotype due to limited BM B lymphopoiesis. Immature splenic T1 and T2 B cells in *lnk*-transgenic mice were enlarged, but were not entered in the G_2/M phase of the cell cycle. These results imply that Lnk also constrains the proliferating ability of peripheral B cells, as well as BM B cell precursors. Apart from FO or MZ B cells, most B cells in $IL\text{-}7^{-/-}$ and conditional *Rag*-knockout mice are enlarged, express activation markers, and show an increased proportion of proliferating cells (37, 38). In contrast, in *lnk*-transgenic mice, enlarged cells were only seen in newly generated T1 and T2 cell compartments. Hence, maturation or compensatory proliferation of peripheral B cells might be perturbed by Lnk overload.

Another possibility is that the phenotype observed in peripheral B cells could be a consequence of unusual selection of B cells that are relatively resistant to Lnk overexpression. Cells which have an advantage in maturation or proliferation might selectively develop in the BM and expand into the periphery in *lnk*-transgenic mice, where they could preferentially differentiate into the B1 and MZ B cell compartments. As shown in recent gene disruption studies, signaling components of B cell receptors, such as tyrosine kinases and coreceptors, survival factors like B cell activating factor from the TNF family/B cell activating factor from the TNF family receptor, components controlling cell migration including protein tyrosin kinase 2 and Lsc (Lbc's second cousin, the murine homolog of human p115 Rho GEF), and transcription factors like, those of the NF-κB family, Aiolos, and recombination signal binding protein-J are all critical for MZ B cell development (3, 39). Cells that could expand carrying high amounts of Lnk might preferentially differentiate in B1 and MZ B cell compartments as a result of altered expression of molecules critical for MZ B cell development.

How does Lnk control lymphocyte proliferation?

Using a c-Kit$^+$ mast cell line, we previously demonstrated that Lnk is tyrosine-phosphorylated by c-Kit and interacts with phosphorylated c-Kit (20). Lnk specifically inhibited c-Kit-mediated signaling for cell growth by attenuating Gab2 (a family member of Gab1, Grb2-associated binder 1) phosphorylation and the subsequent activation of the mitogen-activated protein kinase pathway (20). However, previous studies demonstrated that a c-Kit signal is indispensable for T precursor expansion, whereas B cell generation occurs in the absence of c-Kit (40). Although the impaired expansion of CD4$^-$CD8$^-$ double-negative T precursors in *lnk*-transgenic mice could result from an inhibitory effect of overexpressed Lnk on c-Kit signaling, the observed impairment of B cell production strongly indicates that c-Kit is not the sole target for Lnk. Consistent with this idea, the enhanced hemopoietic ability by *lnk*-deficient hemopoietic precursors was not significantly normalized by attenuating c-Kit signals with the introduction of the heterozygous *W* mutation in the c-Kit locus (20). Flt3/Flk-2 may be involved in such a pathway because it has been shown to support proliferation and differentiation of hemopoietic progenitor cells, while disruption of Flt3/Flk-2 perturbed the production of various blood cell lineages (41). *W/W^{v}flk2*$^{-/-}$ mice show impaired hemopoiesis with severe lymphocytopenia. However, injection of anti-Flt3/Flk-2 Abs into adult mice together with anti-c-Kit Abs does not inhibit B lymphopoiesis, while the treatment severely inhibits erythropoiesis and myelopoiesis (42). Injection of anti-Flt3/Flk-2 Abs into *lnk*$^{-/-}$ mice failed to normalize the B cell overproduction (S. Takaki, unpublished observation). These observations suggest that Flt3/Flk-2 signaling is not likely to be a target affected by Lnk overexpression. Further studies will be required to identify the molecular targets of Lnk and to understand how Lnk regulates the expansion of hemopoietic and lymphoid precursor cells in vivo.

It has been shown that Lnk associates with an actin binding protein, ABP-280 (43). It has also been shown that SH2-B, a member of the Lnk family adaptor proteins, is required for growth hormone induced actin reorganization and regulates cell motility (44, 45). These data suggest that Lnk could associate with an actin-containing complex and may control the actin cytoskeleton during cell division or migration. The relatively maintained splenic architecture in *lnk*-transgenic mice suggests that B cell migration during maturation was unperturbed. However, enlargement of T1 and T2 B cells in transgenic mice might reflect Lnk function in controlling the actin cytoskeleton. In line with the reduction in the fraction of cycling B cells, Lnk might regulate expansion of precursor and mature B cells by preventing both entry into the cell cycle and cell division, in part via effects on cytoskeletal remodeling involving actin.

A mutant form of Lnk lacking the C-terminal tyrosine residue conserved among Lnk family proteins still efficiently inhibited lymphopoiesis in transgenic mice. This is consistent with observations obtained from transfection experiments using the c-Kit$^+$ mast cell line MC9 (20). Although Y536 of Lnk was the main c-Kit target phosphorylation site, SCF-dependent growth of MC9 cells was inhibited by Y536F as well as by wild-type Lnk. In contrast, APS inhibits Janus kinase 2- or platelet-derived growth factor receptor-mediated signaling in combination with c-Cbl, and the phosphorylation of the C-terminal tyrosine is essential for c-Cbl-binding and subsequent APS inhibitory effects (46, 47). This suggests that the Lnk inhibitory function on c-Kit and as yet unidentified signaling cascade(s) is accomplished by Lnk subdomains other than the C-terminal tyrosine and may involve a mechanism unique to Lnk. In contrast to the negative regulatory role of Lnk in lymphopoiesis, positive regulatory roles for SH2-B and APS in signaling via receptors for various cytokines and growth factors have been reported (26–32). Thus, despite the significant structural similarities between Lnk, APS, and SH2-B, their functions appear to be quite different from each other.

In summary, we used transgenic mice overproducing Lnk to demonstrate that this adaptor protein is a critical regulator of lymphocyte production. Expansion of lymphoid precursors was severely impaired in *lnk*-transgenic mice. The skewed peripheral B cell subpopulations, enlarged size of transitional T1 B cells, reduced cycling splenic B cells, and altered humoral immune responses in *lnk*-transgenic mice suggest a potential function for Lnk in peripheral lymphocytes. Thus our results precisely complement studies of *lnk*-deficient mice. In addition, they suggest that Lnk may perform previously undescribed functions in peripheral B cells and during T cell development. Taken together, these genetic studies in mice illuminate the novel negative regulatory mechanism by the Lnk adaptor protein in controlling lymphocyte production and function.

Acknowledgments

We thank H. Kaji and M. Tamura for technical assistance. We thank our colleagues for helpful discussions, and the critical reading of this manuscript.

References

1. Hardy, R. R., C. E. Carmack, S. A. Shinton, J. D. Kemp, and K. Hayakawa. 1991. Resolution and characterization of pro-B and pre-pro-B cell stages in normal mouse bone marrow. *J. Exp. Med. 173:1213.*
2. Oliver, A. M., F. Martin, G. L. Gartland, R. H. Carter, and J. F. Kearney. 1997. Marginal zone B cells exhibit unique activation, proliferative and immunoglobulin secretory responses. *Eur. J. Immunol. 27:2366.*
3. Martin, F., and J. F. Kearney. 2002. Marginal-zone B cells. *Nat. Rev. Immunol. 2:323.*
4. Kantor, A. B., and L. A. Herzenberg. 1993. Origin of murine B cell lineages. *Annu. Rev. Immunol. 11:501.*
5. Martin, F., and J. F. Kearney. 2000. B-cell subsets and the mature preimmune repertoire: marginal zone and B1 B cells as part of a "natural immune memory." *Immunol. Rev. 175:70.*
6. Martin, F., A. M. Oliver, and J. F. Kearney. 2001. Marginal zone and B1 B cells unite in the early response against T-independent blood-borne particulate antigens. *Immunity 14:617.*
7. Healy, J. I., and C. C. Goodnow. 1998. Positive versus negative signaling by lymphocyte antigen receptors. *Annu. Rev. Immunol. 16:645.*
8. Baird, A. M., R. M. Gerstein, and L. J. Berg. 1999. The role of cytokine receptor signaling in lymphocyte development. *Curr. Opin. Immunol. 11:157.*
9. Alberola-Ila, J., S. Takaki, J. D. Kerner, and R. M. Perlmutter. 1997. Differential signaling by lymphocyte antigen receptors. *Annu. Rev. Immunol. 15:125.*
10. Schlessinger, J. 2000. Cell signaling by receptor tyrosine kinases. *Cell 103:211.*
11. Pawson, T., and J. D. Scott. 1997. Signaling through scaffold, anchoring, and adaptor proteins. *Science 278:2075.*
12. Kelly, M. E., and A. C. Chan. 2000. Regulation of B cell function by linker proteins. *Curr. Opin. Immunol. 12:267.*
13. Koretzky, G. A., and P. S. Myung. 2001. Positive and negative regulation of T-cell activation by adaptor proteins. *Nat. Rev. Immunol. 1:95.*

14. Huang, X., Y. Li, K. Tanaka, K. G. Moore, and J. I. Hayashi. 1995. Cloning and characterization of Lnk, a signal transduction protein that links T-cell receptor activation signal to phospholipase Cγ1, Grb2, and phosphatidylinositol 3-kinase. *Proc. Natl. Acad. Sci. USA 92:11618.*
15. Takaki, S., J. D. Watts, K. A. Forbush, N. T. Nguyen, J. Hayashi, J. Alberola-Ila, R. Aebersold, and R. M. Perlmutter. 1997. Characterization of Lnk: an adaptor protein expressed in lymphocytes. *J. Biol. Chem. 272:14562.*
16. Takaki, S., K. Sauer, B. M. Iritani, S. Chien, Y. Ebihara, K. Tsuji, K. Takatsu, and R. M. Perlmutter. 2000. Control of B cell production by the adaptor protein *lnk*: definition of a conserved family of signal-modulating proteins. *Immunity 13:599.*
17. Osborne, M. A., S. Dalton, and J. P. Kochan. 1995. The yeast tribrid system: genetic detection of *trans*-phosphorylated ITAM-SH2-interactions. *BioTechnology 13:1474.*
18. Yokouchi, M., R. Suzuki, M. Masuhara, S. Komiya, A. Inoue, and A. Yoshimura. 1997. Cloning and characterization of APS, an adaptor molecule containing PH and SH2 domains that is tyrosine phosphorylated upon B-cell receptor stimulation. *Oncogene 15:7.*
19. Velazquez, L., A. M. Cheng, H. E. Fleming, C. Furlonger, S. Vesely, A. Bernstein, C. J. Paige, and T. Pawson. 2002. Cytokine signaling and hematopoietic homeostasis are disrupted in Lnk-deficient mice. *J. Exp. Med. 195:1599.*
20. Takaki, S., H. Morita, Y. Tezuka, and K. Takatsu. 2002. Enhanced hematopoiesis by hematopoietic progenitor cells lacking intracellular adaptor protein, Lnk. *J. Exp. Med. 195:151.*
21. Iritani, B. M., K. A. Forbush, M. A. Farrar, and R. M. Perlmutter. 1997. Control of B cell development by Ras-mediated activation of Raf. *EMBO J. 16:7019.*
22. Garvin, A. M., K. M. Abraham, K. A. Forbush, A. G. Farr, B. L. Davison, and R. M. Perlmutter. 1990. Disruption of thymocyte development and lymphomagenesis induced by SV40 T-antigen. *Int. Immunol. 2:173.*
23. Uehara, S., Y. Hitoshi, F. Numata, M. Makino, M. Howard, T. Mizuochi, and K. Takatsu. 1994. An IFN-γ-dependent pathway plays a critical role in the pathogenesis of murine immunodeficiency syndrome induced by LP-BM5 murine leukemia virus. *Int. Immunol. 6:1937.*
24. Li, Y. S., R. Wasserman, K. Hayakawa, and R. R. Hardy. 1996. Identification of the earliest B lineage stage in mouse bone marrow. *Immunity 5:527.*
25. Iseki, M., S. Takaki, and K. Takatsu. 2000. Molecular cloning of the mouse APS as a member of the Lnk family adaptor proteins. *Biochim. Biophys. Acta 272:45.*
26. Qian, X., A. Riccio, Y. Zhang, and D. D. Ginty. 1998. Identification and characterization of novel substrates of Trk receptors in developing neurons. *Neuron 21:1017.*
27. Rui, L., and C. Carter-Su. 1999. Identification of SH2-Bβ as a potent cytoplasmic activator of the tyrosine kinase Janus kinase 2. *Proc. Natl. Acad. Sci. USA 96: 7172.*
28. Rui, L., J. Herrington, and C. Carter-Su. 1999. SH2-B is required for nerve growth factor-induced neuronal differentiation. *J. Biol. Chem. 274:10590.*
29. Ahmed, Z., and T. S. Pillay. 2001. Functional effects of APS and SH2-B on insulin receptor signalling. *Biochem. Soc. Trans. 29:529.*
30. Qian, X., and D. D. Ginty. 2001. SH2-B and APS are multimeric adapters that augment TrkA signaling. *Mol. Cell Biol. 21:1613.*
31. Yousaf, N., Y. Deng, Y. Kang, and H. Riedel. 2001. Four PSM/SH2-B alternative splice variants and their differential roles in mitogenesis. *J. Biol. Chem. 276: 40940.*
32. O'Brien, K. B., J. J. O'Shea, and C. Carter-Su. 2002. SH2-B family members differentially regulate JAK family tyrosine kinases. *J. Biol. Chem. 277:8673.*
33. Ohtsuka, S., S. Takaki, M. Iseki, K. Miyoshi, N. Nakagata, Y. Kataoka, N. Yoshida, K. Takatsu, and A. Yoshimura. 2002. SH2-B is required for both male and female reproduction. *Mol. Cell Biol. 22:3066.*
34. Abraham, K. M., S. D. Levin, J. D. Marth, K. A. Forbush, and R. M. Perlmutter. 1991. Delayed thymocyte development induced by augmented expression of $p56^{lck}$. *J. Exp. Med. 173:1421.*
35. Levin, S. D., S. J. Anderson, K. A. Forbush, and R. M. Perlmutter. 1993. A dominant-negative transgene defines a role for $p56^{lck}$ in thymopoiesis. *EMBO J. 12:1671.*
36. Alberola-Ila, J., K. A. Forbush, R. Seger, E. G. Krebs, and R. M. Perlmutter. 1995. Selective requirement for MAP kinase activation in thymocyte differentiation. *Nature 373:620.*
37. Carvalho, T. L., T. Mota-Santos, A. Cumano, J. Demengeot, and P. Vieira. 2001. Arrested B lymphopoiesis and persistence of activated B cells in adult interleukin $7^{-/-}$ mice. *J. Exp. Med. 194:1141.*
38. Hao, Z., and K. Rajewsky. 2001. Homeostasis of peripheral B cells in the absence of B cell influx from the bone marrow. *J. Exp. Med. 194:1151.*
39. Tanigaki, K., H. Han, N. Yamamoto, K. Tashiro, M. Ikegawa, K. Kuroda, A. Suzuki, T. Nakano, and T. Honjo. 2002. Notch-RBP-J signaling is involved in cell fate determination of marginal zone B cells. *Nat. Immunol. 3:443.*
40. Takeda, S., T. Shimizu, and H. R. Rodewald. 1997. Interactions between c-*kit* and stem cell factor are not required for B-cell development in vivo. *Blood 89:518.*
41. Mackarehtschian, K., J. D. Hardin, K. A. Moore, S. Boast, S. P. Goff, and I. R. Lemischka. 1995. Targeted disruption of the *flk2/flt3* gene leads to deficiencies in primitive hematopoietic progenitors. *Immunity 3:147.*
42. Ogawa, M., S. Sugawara, T. Kunisada, T. Sudo, S. Hayashi, S. Nishikawa, and H. Kodama. 1998. Flt3/Flk-2 and c-Kit are not essential for the proliferation of B lymphoid progenitor cells in the bone marrow of the adult mouse. *Exp. Hematol. 26:478.*
43. He, X., Y. Li, J. Schembri-King, S. Jakes, and J. Hayashi. 2000. Identification of actin binding protein, ABP-280, as a binding partner of human Lnk adaptor protein. *Mol. Immunol. 37:603.*
44. Herrington, J., M. Diakonova, L. Rui, D. R. Gunter, and C. Carter-Su. 2000. SH2-B is required for growth hormone-induced actin reorganization. *J. Biol. Chem. 275:13126.*
45. Diakonova, M., D. R. Gunter, J. Herrington, and C. Carter-Su. 2002. SH2-Bβ is a Rac-binding protein that regulates cell motility. *J. Biol. Chem. 277:10669.*
46. Yokouchi, M., T. Wakioka, H. Sakamoto, H. Yasukawa, S. Ohtsuka, A. Sasaki, M. Ohtsubo, M. Valius, A. Inoue, S. Komiya, and A. Yoshimura. 1999. APS, an adaptor protein containing PH and SH2 domains, is associated with the PDGF receptor and c-Cbl and inhibits PDGF-induced mitogenesis. *Oncogene 18:759.*
47. Wakioka, T., A. Sasaki, K. Mitsui, M. Yokouchi, A. Inoue, S. Komiya, and A. Yoshimura. 1999. APS, an adaptor protein containing Pleckstrin homology (PH) and Src homology-2 (SH2) domains inhibits the JAK-STAT pathway in collaboration with c-Cbl. *Leukemia 13:760.*

MOLECULAR AND CELLULAR BIOLOGY, May 2002, p. 3066–3077 Vol. 22, No. 9
0270-7306/02/$04.00+0 DOI: 10.1128/MCB.22.9.3066–3077.2002

SH2-B Is Required for Both Male and Female Reproduction

Satoshi Ohtsuka,[1] Satoshi Takaki,[2] Masanori Iseki,[2] Kanta Miyoshi,[3] Naomi Nakagata,[4] Yuki Kataoka,[5] Nobuaki Yoshida,[5] Kiyoshi Takatsu,[2] and Akihiko Yoshimura[1,3]*

Division of Molecular Genetics, Institute of Life Science, Kurume University, Kurume 839-0861,[1] Division of Immunology, Department of Microbiology and Immunology,[2] and Laboratory of Gene Expression and Regulation, Center for Experimental Medicine,[5] Institute of Medical Science, The University of Tokyo, Minato-ku 108-8639, Division of Molecular and Cellular Immunology, Medical Institute of Bioregulation, Kyushu University, Higashi-ku, Fukuoka 812-8582,[3] and Division of Reproductive Engineering, Center for Animal Resources & Development, Kumamoto University, Kumamoto 860-0811,[4] Japan

Received 2 October 2001/Returned for modification 6 November 2001/Accepted 7 February 2002

Many growth factors and hormones modulate the reproductive status in mammals. Among these, insulin and insulin-like growth factor I (IGF-I) regulate the development of gonadal tissues. SH2-B has been shown to interact with insulin and IGF-I receptors, although the role of SH2-B in these signals has not been clarified. To investigate the role of SH2-B, we generated mice with a targeted disruption of the SH2-B gene. Both male and female SH2-B$^{-/-}$ mice showed slight retardation in growth and impaired fertility. Female knockout mice possess small, anovulatory ovaries with reduced numbers of follicles and male SH2-B$^{-/-}$ mice have small testes with a reduced number of sperm. SH2-B$^{-/-}$ cumulus cells do not respond to either follicle-stimulating hormone or IGF-I. These data suggest that SH2-B plays a critical role in the IGF-I-mediated reproductive pathway in mice.

Cytokine and growth factor receptors trigger multiple signaling cascades that regulate cell growth and differentiation. Many growth factor receptors have a protein tyrosine kinase domain in their cytoplasmic region (receptor tyrosine kinase [RTK]). In contrast, cytokine receptors, such as those for interleukins, interferons, and colony-stimulating factors, do not have an intrinsic kinase domain but instead constitutively associate with Janus tyrosine kinases (JAKs). Binding of growth factors and cytokines to their cognate receptors induces the homo- and heterodimerization of the receptors, an event which positions the kinase domains close to each other. This leads to transphosphorylation and thereby activation of RTKs and receptor-associated JAKs. The activated kinases further phosphorylate other tyrosine residues in the cytoplasmic region, where various signaling molecules containing Src homology 2 (SH2) or phosphotyrosine binding domains are recruited. As a consequence, these recruited adaptor molecules contribute to specification and amplification of signaling downstream of the receptors. Lnk family proteins, including Lnk, APS, and SH2-B, are some of these adaptor molecules (39).

SH2-B was originally identified by using a yeast trihybrid system as a protein associated with an immunoreceptor tyrosine-based activation motif in the high-affinity immunoglobulin E (IgE) receptor Fcε-RI (29). SH2-B contains a proline-rich domain, a Pleckstrin homology (PH) domain, and an SH2 domain. APS was initially cloned from a B-cell cDNA library using a yeast two-hybrid screening with the c-Kit RTK as bait, and it was shown to associate with a B-cell receptor (44). Lnk was cloned from a rat lymph node cDNA library and was shown to participate in T-cell signaling (20, 38, 39). In Lnk$^{-/-}$ mice, T-cell development was unaffected, but pre-B and immature B cells accumulated in the spleen and in the bone marrow, thereby indicating that the Lnk protein negatively regulates the production of pro-B cells and c-Kit (39, 40).

Recently, SH2-B was reported to mediate signaling through many cytokine and growth factor receptors, including growth hormone (GH), insulin, insulin-like growth factor I (IGF-I), platelet-derived growth factor (PDGF), and nerve growth factor (NGF) receptors (23, 31–33, 36, 37, 47). SH2-B has been shown to mediate mitogenic signals as well as ERK activation through these receptors (44, 45). A variant form of SH2-B, SH2-Bβ, was reported to be a substrate of the tyrosine kinase JAK2 and to potentiate JAK2 kinase activity (34, 35). However, these studies were performed using an in vitro cultured cell system, and the conclusions were obtained from the overexpression of wild-type or domain negative forms. To clarify the physiological role of SH2-B adaptor molecules, we used gene targeting to acquire mice lacking the SH2-B gene. SH2-B$^{-/-}$ mice displayed normal development of lymphoid organs but decreased body weight and developmental defects in gonadal organs similar to the phenotype seen in mice with IGF-I or follicle-stimulating hormone receptor (FSH-R) deficiencies (24, 26). We propose that while SH2-B is dispensable for JAK2 activation, it does play an important role in the IGF-I pathway that up-regulates FSH-R levels in vivo.

MATERIALS AND METHODS

Generation of SH2-B$^{-/-}$ mice. Genomic clones of the SH2-B locus, including all exons, were isolated from a 129sv mouse strain genomic library (Stratagene). The targeting vector was constructed by replacing the second through the eighth exons of the SH2-B gene with a PGK-NEO cassette, preserving 8.0-kb (left arm) and 3.8-kb (right arm) flanks of homologous sequences (see Fig. 1). The diphtheria toxin A gene was inserted for negative selection. Homologous recombination in murine embryonic stem cells was performed as described previously (19) and was confirmed by Southern blot analysis (probes are shown below in Fig.

* Corresponding author. Mailing address: Division of Molecular and Cellular Immunology, Medical Institute of Bioregulation, Kyushu University, Maidashi 3-1-1, Higashi-ku, Fukuoka 812-8582, Japan. Phone: 81-92-642-6822. Fax: 81-92-642-6825. E-mail: yakihiko@bioreg.kyushu-u.ac.jp.

1). Chimeric mice were mated with wild-type C57BL/6 mice to generate heterozygous F_1 progeny. The F_1 progeny were intercrossed to acquire F_2 progeny for analysis.

Flow cytometric analysis. Single-cell suspensions of lymphocytes from bone marrow, thymus, spleen, or lymph nodes were prepared. Red blood cells were lysed and removed using 0.15 M NH_4Cl, 1.0 mM $KHCO_3$, 0.1 mM EDTA (pH 7.2) prior to staining. Predetermined optimal concentrations of the respective antibodies were used to stain 0.5×10^6 to 1.0×10^6 cells at 4°C for 20 min. Cells were washed and analyzed on a FACScan instrument (Becton Dickinson, Mountain View, Calif.) using CellQuest software (Becton Dickinson). The following monoclonal antibodies (MAbs) were used: fluorescein isothiocyanate (FITC)-conjugated anti-CD8 (53-6.7), phycoerythrin (PE)-conjugated anti-CD4 (RM4-5), biotin-conjugated anti-CD3ε (145-2C11), PE- or biotin-conjugated anti-CD43 (S7), PE-conjugated anti-Gr-1 (RB6-8C5), and FITC-conjugated anti-Mac-1 (M1/70) (all purchased from Pharmingen, San Diego, Calif.); FITC- or PE-conjugated anti-B220 (RA3-6B2) (Caltag Laboratories, Burlingame, Calif.); biotin-conjugated anti-IgD (CS/15; gift from K. Miyake, Tokyo, Japan). FITC- or PE-conjugated $F(ab')_2$ fragments of polyclonal anti-IgM were purchased from Caltag Laboratories, and PE- or TRI-COLOR-conjugated streptavidin (Caltag Laboratories) was used to reveal biotin-coupled antibody staining.

Lymphocyte proliferation and cytokine production. Splenic B cells were purified using a MACS system (Miltenyi Biotec, Bergisch Gladbach, Germany) after incubation with biotin-conjugated anti-CD43 and streptavidin-coupled microbeads (Miltenyi Biotec). B cells (10^5) were cultivated in 0.2 ml of RPMI 1640 medium supplemented with 10% fetal calf serum (FCS), 50 μM 2-mercaptoethanol, 100 U of penicillin/ml, and 100 μg of streptomycin/ml in a 96-well plate. Cells were stimulated with anti-mouse IgM $F(ab')_2$ (Organon Teknika, Durham, N.C.), interleukin-4 (IL-4), 10 μg of lipopolysaccharide (Difco Laboratories, Detroit, Mich.) per ml, or 3 μg of anti-CD40 (HM40-3; Pharmingen) per ml. Cells were pulse-labeled with [^{3}H]thymidine (0.2 μCi per well) during the last 16 h of a 66-h culture period, and the incorporated [^{3}H]thymidine was measured using a Matrix 96 Direct Beta Counter (Packard, Meriden, Conn.).

For T-cell proliferation assays, splenocytes (10^6) were cultured in 0.2 ml of medium in a 96-well plate in the presence of various concentrations of anti-CD3ε (145-2C11). Cells were pulse-labeled with [^{3}H]thymidine (0.2 μCi per well) during the last 8 h of a 48-h culture period, and the incorporated [^{3}H]thymidine was measured.

For the assessment of cytokine production, splenocytes (10^6) were cultured in 0.2 ml of medium in the presence of 10 μg of anti-CD3ε/ml for 48 h. Culture supernatants were collected, and the levels of IL-2 and IL-4 in the supernatants were measured by enzyme-linked immunosorbent assay (ELISA) as described elsewhere (41). All of the MAbs used for the capture and detection of cytokines were purchased from Pharmingen.

Serology. Concentrations of each immunoglobulin isotype in serum were determined in 6-week-old mice by isotype-specific ELISA (41). To measure production of the antibodies against thymus-independent antigens, mice were intraperitoneally injected with 10 μg of trinitrophenol (TNP)-Ficoll in saline and were bled on day 10 after injection. Serial dilutions of serum were analyzed for TNP-specific immunoglobulin isotypes by ELISA using dinitrophenol (DNP)-coupled bovine serum albumin (BSA), which cross-reacts with anti-TNP antibodies) as a capture reagent. To examine the response against thymus-dependent antigens, mice were immunized intraperitoneally with 100 μg of BSA in a 1:1 homogenate of incomplete Freund's adjuvant (Nacalai Tesque, Kyoto, Japan) and saline. A booster dose of 100 μg of BSA in saline was given on day 20. Mice were bled on day 30 and the presence of anti-BSA antibodies in each immunoglobulin subclass was determined using a BSA-specific ELISA.

Mast cell cultures and functional assays. Bone marrow-derived mast cells (BMMCs) were obtained from a culture of bone marrow cells in RPMI 1640 supplemented with 5 ng of murine IL-3/ml (Pepro Tech EC), 8% FCS, nonessential amino acids (Gibco BRL), 100 IU of penicillin/ml, 100 μg of streptomycin/ml, and 10 μM 2-mercaptoethanol. We used BMMCs cultured for 4 to 10 weeks for all studies. BMMCs were cultured in 96-well plates (5×10^4 cells; 0.2 ml/well) for 48 h in RPMI 1640 supplemented with 8% FCS and various concentrations of stem cell factor (SCF) or IL-3 as indicated. [^{3}H]thymidine (0.2 μCi per well) was added 12 h before cells were harvested, and the incorporated [^{3}H]thymidine was measured. BMMCs were sensitized with anti-DNP IgE by incubation in cultured supernatants of Igel α2(15.3) hybridoma cells at 37°C for 1 h, after which they were washed, resuspended in Tyrode's buffer (10 mM HEPES [pH 7.4], 130 mM NaCl, 5 mM KCl, 1.4 mM $CaCl_2$, 1 mM $MgCl_2$, 5.6 mM glucose, and 0.1% BSA), and left unstimulated or stimulated with DNP-BSA for 1 h at 37°C. The degranulation was evaluated by measuring the amount of granular enzyme β-hexosaminidase released from cells. The enzymatic activities of β-hexosaminidase in supernatants and cell pellets solubilized with 0.5% Triton X-100 and Tyrode's buffer were measured with *p*-nitrophenyl *N*-acetyl-β-D-glucosaminide (Sigma Chemical Co.) in 0.1 M sodium citrate (pH 4.5) for 90 min at 37°C. The reaction was stopped by adding 0.2 M glycine (pH 10.7). The product 4-*p*-nitrophenol was detected by absorbance at 405 nm. Percentages of degranulation were calculated by dividing absorbance in the supernatants by total absorbance in the supernatants and cell pellets.

Sperm assay. For sperm analysis, we collected sperm from the epididymides of SH2-B-null and wild-type mice as described previously (19). The sperm was incubated in R18S3 medium (180 mg of Raffinose/ml and 30 mg of skim milk/ml) for 1 h in a 5% CO_2 atmosphere equilibrated with 5% CO_2. The sperm were diluted 1:100 with isotonic saline, and a phase-contrast microscope was used to count the sperm and to evaluate the morphology. We followed the procedure of the World Health Organization laboratory manual for the examination of human semen and semen-cervical mucus interaction to measure sperm motility (43a).

IVF. For in vitro fertilization (IVF), we collected sperm from the epididymides of SH2-B-null and wild-type males as described previously (19). Then, we incubated the sperm in HTF medium supplemented with 0.75 μg of penicillin G/ml and 0.5 μg of streptomycin/ml in a 5% CO_2 atmosphere, equilibrated with 5% CO_2, for at least 1 h for capacitation. Females were treated to induce superovulation, and oocytes were collected from the ampullae of their oviducts. Only fully matured oocytes, as confirmed by the first polar body release, were used for IVF experiments. We excluded oocytes with no first polar body. Oocytes were treated with 0.1% hyaluronidase to remove surrounding granulosa and cumulus cells. Thereafter, 10 μl of the sperm suspension solution was transferred into the oocytes in saline followed by incubation for 24 h under 5% CO_2 at 37°C. After 24 h, these inseminated eggs were beginning cleavage, and the number of two-cell-stage eggs was counted. These two-cell-stage embryos were transplanted into ICR mice (purchased from Japan SLC Inc.) as described previously (19).

COC expansion assay. Briefly, 48 h after administration of pregnant mare serum gonadotropin (PMSG), cumulus cell-oocyte complexes (COCs) were collected from the oviduct ampullae of wild-type and SH2-$B^{-/-}$ mice sacrificed by cervical dislocation. The large Graafian follicles were punctured with 27-gauge needles, and the COCs were extruded into Waymouth's medium MB752/1 (Gibco BRL). Because exposure to IGF-I and FSH leads to drastic changes in cumulus cells due to the hyaluronidase hypersensitivity of the cumulus oophori, we cultured COCs in Waymouth's medium MB752/1 containing 3 mg of BSA (Gibco BRL) per ml rather than FCS (control), in order to reduce hyaluronic acid synthesis and to avoid this effect of IGF-1 in the serum (13). Cultures were maintained in a humidified atmosphere of 5% O_2–5% CO_2–90% N_2 at 37°C for 24 h. Other COCs were cultured in Waymouth's medium containing 3 mg of BSA/ml and 1 μg of highly purified rat FSH (Biogenesis Ltd.) per ml, or 3 mg of BSA/ml plus 10 ng of IGF-I (Pepro Tech EC, Ltd) per ml, into which 1 μg of highly purified mouse FSH/ml was added after 4 h. For immunoblotting with anti-phosphotyrosine and anti-phosphorylated mitogen-activated protein (MAP) kinase (ERK2) antibodies, COCs were incubated with 100 ng of IGF-1/ml for 20 min and then cell extracts were prepared.

Northern hybridization and RT-PCR. Total RNA was extracted from tissues and cells using Trizol reagent (Gibco BRL). Total RNA (10 μg) was separated on 1.0% agarose gels containing 2.4% formaldehyde and then transferred to positively charged nylon membranes. After fixation under calibrated UV irradiation, the membranes were hybridized with [^{32}P]CTP-labeled cDNA probes as described previously (44). SH2-B probe (334 bp) was obtained by PCR from a mouse testis cDNA library and primer sets (5′-GAGGAAGTCGCTTGGAGT TCTTTGTAC-3′ and 5′-TCCTGGCTAGGCAGACTCTCTGAATGA-3′). FSH-R cDNA (about 2 kb) was obtained by PCR using ovary cDNA and primer sets (5′-ATGGCCTGGCTCCTGGTCTCCTTGCT-3′ and 5′-GAGGGACAAGCA CGTAACTATTGGTGACT). To detect SH2-B, APS, and Lnk mRNA in mast cells and splenocytes, standard reverse transcription-PCR (RT-PCR) was performed using a Standard GeneAmp RNA PCR kit (PE Biosystems) according to the manufacturer's instructions. The following primer sets were used: SH2-B (about 150 bp), 5′-TCTACTATTACTGATGTCCGCACAGCC-3′ and 5′-TGT ACTCTGAAGGGCCTTCTACCTTAA-3′; Lnk (930 bp), 5′-ATGCCTGACA ACCTCTACAC-3′ and 5′-ATTCACACGTCTGCCTCTCT-3′; APS (530 bp), 5′-GAAAGGGATTCTGGCTGCGTAACA and 5′-ATCCACACAGCCCTGG ATGTCAGC. PCR primers for SH2-B splice variants have been described by Yousaf et al. (46).

Immunoblotting and immunostaining. For immunoblotting, total cell extracts were resolved by sodium dodecyl sulfate-polyacrylamide gel electrophoresis (SDS-PAGE), and proteins were detected by immunoblotting as described previously (44). Anti-phospho-STAT5 and phospho-ERK2-specific antibodies were purchased from Cell Signaling and Upstate Biotechnology.

An anti-SH2-B antibody (G-17) which reacts with the N-terminal region of the SH2-B protein was purchased from Santa Cruz Biotechnology, Inc., and an

anti-murine APS antibody was affinity purified as described previously (21). For immunofluorescence microscopy, tissues were fixed overnight in 4% paraformaldehyde and embedded in optimal cutting temperature compound. Tissues were cryostat sectioned to a 10-μm thickness and incubated with a 1:100 dilution of anti-SH2-B antibody, followed by staining with a FITC-conjugated anti-goat IgG antibody. Then, the samples were examined with fluorescent microscopy. For immunohistochemistry, tissues were fixed with 10% buffered formalin, dehydrated through a graded series of alcohol, cleared in xylene, and embedded in paraffin. Paraffin blocks were sectioned at 3-μm thickness. Slides were incubated with a 1:100 dilution of anti-APS antibody and stained with a peroxidase-conjugated anti-rabbit IgG using an Envision+ kit (Dako, Carpinteria, Calif.). The samples were then stained with Mayer's hematoxylin.

RESULTS

Generation of SH2-B knockout (KO) mice. To clarify the physiological role of SH2-B, we developed mice with a targeted disruption in the SH2-B gene locus. Since the PH and SH2 domains are predicted to be essential for SH2-B to function as an adaptor protein, the exons encoding these domains (second to eighth exons) were deleted (Fig. 1A). For genotyping of the F_2 offspring generated by intercrossing the F_1 heterozygotes, Southern blot analysis was carried out. This revealed a ratio of offspring within the Mendelian expectation for transmission (1 (+/+):2 (+/−):1 (−/−) (Fig. 1B). The disruption of SH2-B gene expression was confirmed by Northern blot analysis (Fig. 1C). SH2-B homozygotes exhibited no significantly abnormal appearance at birth.

At age 2 to 6 weeks, the body weight of the SH2-B$^{-/-}$ mice was 60 to 80% that of wild-type littermates (Fig. 1D). In this period, SH2-B-null mice showed postnatal growth retardation and proportionate dwarfism. However, the size and weight of SH2B$^{-/-}$ mice became similar to that of wild-type mice after 6 to 10 weeks. These phenotypes may be related to a reduced response to GH or IGF-I. Occasionally, some of the SH2-B-null mice died shortly after birth (8 out of 78 SH2-B$^{-/-}$ pups), although the cause of death was not clear.

Normal development and function of T, B, and mast cells in SH2-B KO mice. We initially investigated SH2-B mRNA distribution in wild-type mice by using Northern blot analysis (Fig. 1E). SH2-B mRNA is widely expressed in most organs, but the strongest expression was observed in the thymus (lane 3), lymph node (lane 8), and spleen (lane 9), in addition to the brain (lanes 1 and 2), ovary (lane 12), and testis (lane 13). SH2-B has been shown to be an activator of JAK2 (34), which is essential for cytokine signal transduction and hematopoiesis (30). We therefore analyzed the development and function of lymphocytes and myeloid cells in SH2B$^{-/-}$ mice. The cellularity in the bone marrow, thymus, spleen, and lymph nodes was grossly normal in SH2-B$^{-/-}$ mice (data not shown), and B- and T-cell development was also normal as assessed by flow cytometry (Fig. 2). The cellular distribution in each lymphoid organ was comparable to that of normal mice, and expression levels of various surface proteins on lymphocytes or myeloid cells were also comparable.

We then examined SH2-B$^{-/-}$ lymphocyte functions in vitro and in vivo. The proliferative responses of B cells induced by various stimuli were normal (Fig. 3A). SH2-B$^{-/-}$ T cells proliferated normally upon stimulation with anti-CD3 and produced normal levels of IL-2 and IL-4 (Fig. 3B and C). SH2-B$^{-/-}$ mice had normal antibody responses against immunization with both a thymus-independent antigen, TNP-Ficoll, and a thymus-dependent antigen, BSA (Table 1). Thus, SH2-B seems dispensable for lymphocyte development and steady-state hematopoiesis and for functions of lymphocytes and antigen-presenting cells.

APS and Lnk, members of the adaptor protein family to which SH2-B belongs, have been implicated in functioning in the c-Kit signaling pathway (39, 40, 44). SH2-B was originally reported to be a possible adaptor protein that binds to the immunoreceptor tyrosine-based activation motif of FcεRI in mast cells (29). We therefore asked if loss of SH2-B would affect the mast cell function largely regulated by c-Kit and FcεRI signaling. IL-3-dependent BMMCs were established from SH2-B$^{-/-}$ mice and their normal littermates. As shown in Fig. 4A, SH2-B was expressed in wild-type BMMCs, and Lnk and APS was expressed at comparable levels in both wild-type and SH2-B-null BMMCs. BMMCs of both origins expressed c-Kit in comparable amounts (data not shown), and they proliferated equally in response to IL-3 or SCF (Fig. 4B). Activation (phosphorylation) of STAT5 (a substrate of JAK2), and ERK2 MAP kinase (downstream of JAK2) was similarly induced in response to IL-3 in wild-type and SH2-B$^{-/-}$ mast cells (Fig. 4C). Expression levels of high-affinity FcεR assessed by the binding of IgE MAb were also comparable between SH2-B$^{-/-}$ and normal BMMCs (data not shown), and degranulation was similarly induced by cross-linking of FcεRI in BMMCs from both sources (Fig. 4D). These results indicate that SH2-B deficiency does not compromise mast cell function.

Impaired fertility in SH2-B KO mice. Although offspring were born normally from intercrosses of heterozygotes, few offspring were born following incrosses of homozygotes (Fig. 5A). Only 1 of 25 breeding pairs of SH2-B$^{-/-}$ male and SH2-B$^{-/-}$ female mice produced offspring. Both SH2-B$^{-/-}$ male and female mice also showed reduced fertility when mated with wild-type mice (Fig. 5A). We monitored SH2-B$^{-/-}$ incrossed females daily for the presence of vaginal plugs, an indication that copulation has occurred. It took a much longer time after mating for vaginal plugs to be observed in the SH2-B$^{-/-}$ mice than it did following wild-type matings (5.3 ± 1.3 days for wild-type female mice [n = 13], and 31.8 ± 5.8 days or no plugs for female SH2-B$^{-/-}$ mice [n = 22]).

To investigate the cause of this phenotype, we immunohistochemically stained gonadal tissues (testis and ovary) from wild-type mice (Fig. 5B). SH2-B was localized in Leydig cells of the testis and stromal cells of the ovary. Therefore, reduced fertility of SH2-B-null mice might be related to the immaturity or deficiency of the reproductive systems. Dissection of SH2-B$^{-/-}$ mice revealed hypoplasia of the testis and ovary (Fig. 5C), even though their body weights were almost the same as those in controls at 10 weeks of age. Although the seminal vesicle and prostate gland (so-called accessory reproductive organs) were normal (data not shown), the testes and ovaries from SH2-B$^{-/-}$ mice showed size and weight reductions of approximately 50% compared to those from the wild-type and heterozygous controls.

Ovarian sections from SH2-B$^{-/-}$ mice revealed evidence of anovulation, based on the lack of antral follicles and the presence of many preantral follicles (Fig. 6A). The uterine tubules in SH2-B$^{-/-}$ mice were also immature compared to those in wild-type mice (Fig. 6B). We also observed a significant decrease in the number of ovulated oocytes under natural con-

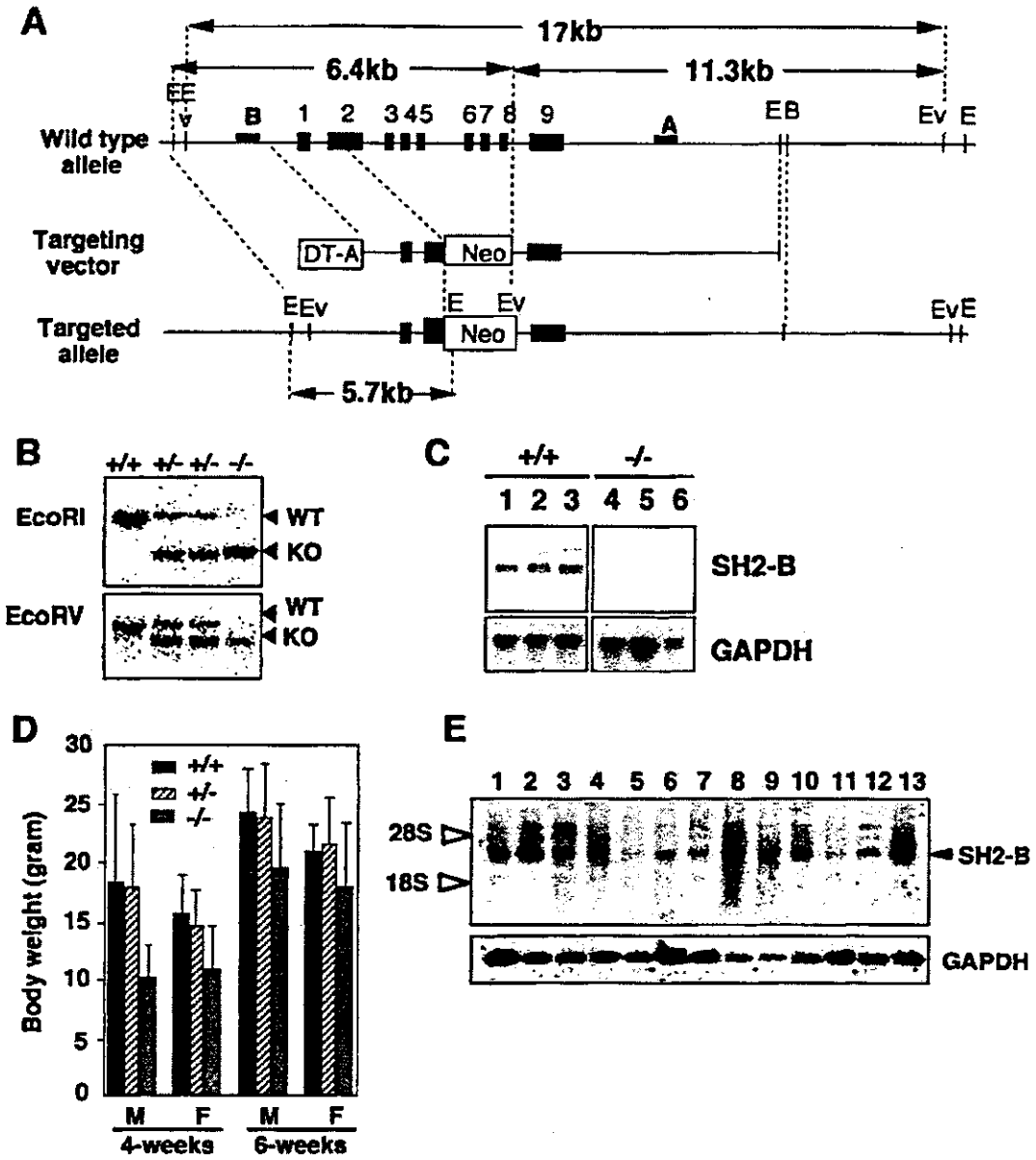

FIG. 1. Generation of SH2-B-deficient mice. (A) Schematic representations of wild-type and mutant loci of the SH2-B gene together with the targeting vector. Exons for genes encoding SH2-B are represented by black boxes. The neomycin resistance gene (Neo) driven by the phosphoglycerate kinase promoter and the gene coding for diphtheria toxin fragment A (DT-A) driven by an MC1 promoter are indicated by white boxes. The 5′ and 3′ probes used for Southern blotting are indicated by a solid bar. The *Eco*RI- and *Eco*RV-digested genomic DNA fragments were detected by probe B and probe A, respectively. Restriction sites: E, *Eco*RI; Ev, *Eco*RV; B, *Bam*HI. (B) Representative Southern blot analysis with *Eco*RV-digested and *Eco*RI-digested DNA. Of 138 offspring from crosses between F_2 heterozygous mice, 35 were +/+, 70 were +/−, and 33 were −/−. (C) Northern blot analysis of total RNA from wild-type (lanes 1 to 3) and SH2-B$^{-/-}$ (lanes 4 to 6) mice showed no SH2-B mRNA expression in SH2-B$^{-/-}$ mice. Lanes 1 and 4, cerebrum; lanes 2 and 5, cerebellum; lanes 3 and 6, testis. Glyceraldehyde-3-phosphate dehydrogenase (GAPDH) levels are shown as an internal control. (D) Growth of SH2-B KO mice. The body weights of 4- and 6-week-old male (M) and female (F) mice were measured. The number of analyzed mice are as follows: 4-week-old male mice (+/+, 11; +/−, 15; −/−, 12); 4-week-old female mice (+/+, 7; +/−, 15; −/−, 9); 6-week-old male mice (+/+, 13; +/−, 15; −/−, 9); and 6-week-old female mice (+/+, 8; +/−, 14; −/−, 8). Results are shown as mean ± standard error of the mean. (E) Tissue distribution of SH2-B mRNA. Ten micrograms of total RNA was loaded in each lane. Lanes: 1, cerebrum; 2, cerebellum; 3, thymus; 4, skeletal muscle; 5, stomach; 6, small intestine; 7, colon; 8, lymph node; 9, spleen; 10, kidney; 11, liver; 12, ovary; 13, testis.

ditions in the mutant mice (Fig. 6E). These observations suggest a dysregulation of the estrous cycle. In the testis, the number of Leydig cells was also reduced in SH2-B$^{-/-}$ male mice compared with wild-type controls (Fig. 6C). Epididymides were also immature, and the number of sperm collected from the epididymides of SH2-B$^{-/-}$ mice was significantly reduced (Fig. 6D and F). The sperm from SH2-B-null mice had an abnormal morphological appearance and much-re-

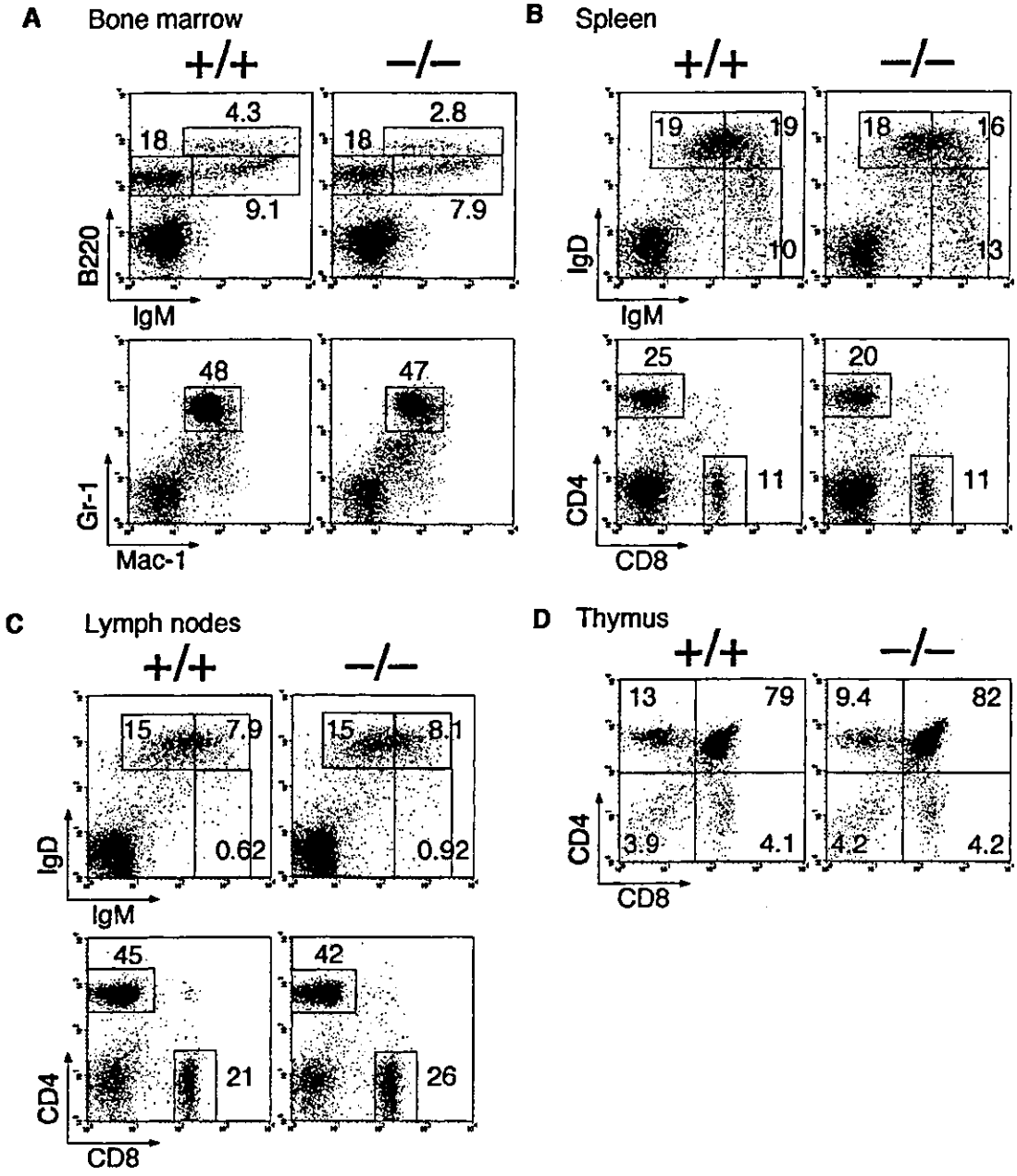

FIG. 2. Normal lymphocyte development in SH2-B$^{-/-}$ mice. Representative two-color fluorescence plots showing expression of B220 and IgM (measuring B-cell development) or Gr-1and Mac-1 (granulocytes and macrophages) on bone marrow cells (A), IgD and IgM (B-cell development), or CD4 and CD8 (T-cell development) on splenocytes and lymph node cells (B, C), and CD4 and CD8 on thymocytes (D). Percentages represent the fractions of the total gated live cells that fall into the indicated boxes. Cellular distribution in each lymphoid organ and expression levels of various surface proteins on lymphocytes or myeloid cells were comparable between SH2-B$^{-/-}$ mice and normal littermates.

duced motility compared to sperm from wild-type mice (data not shown).

To determine which splice variant of SH2-B is expressed in gonadal tissues, we performed RT-PCR with primers which distinguish between the four variants to amplify short PCR fragments, as described by Yousaf et al. (46) (Fig. 6G). Consistent with their data, β and γ isoforms were predominately expressed in the ovary and testis, while levels of α and δ isoforms were low. To determine if APS is expressed in compensation in the ovary and testis, we examined APS expression using RT-PCR (Fig. 6G) as well as immunohistochemistry (Fig. 6H; data on the ovary are not shown). We found no overexpression of APS in SH2-B$^{-/-}$ mice. Immunohistochemistry revealed that APS protein is expressed in seminiferous tubules containing spermatogonia in the testis (Fig. 6H), while SH2-B is expressed in Leydig cells (Fig. 5B). SH2-B and APS

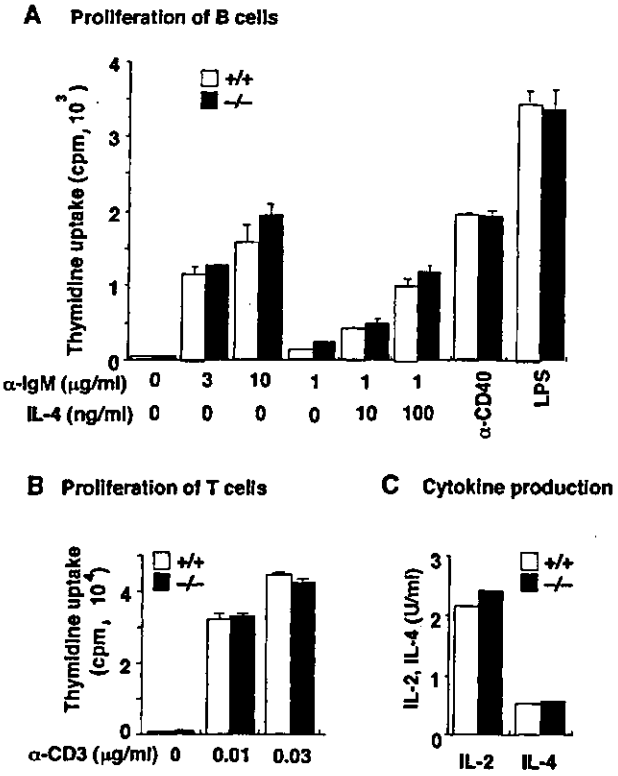

FIG. 3. Normal proliferative response and cytokine production by SH2-B$^{-/-}$ lymphocytes. (A) Proliferation of splenic B cells induced by anti-IgM, anti-CD40, or lipopolysaccharide (LPS). Splenic B cells from SH2-B$^{-/-}$ mice or wild-type littermates were stimulated with indicated stimuli, and proliferation was measured on day 3 by [^{3}H]thymidine incorporation. The values are the mean counts per minute $\times 10^{-3}$ ($\pm$ standard deviation [SD]) of triplicate determinations. Representative results of three independent experiments are shown. (B) Splenocytes from SH2-B$^{-/-}$ mice or wild-type littermates were stimulated with the indicated concentrations of anti-CD3ε, and proliferation was measured on day 2. The values are the mean counts per minute $\times 10^{-3}$ ($\pm$ SD) of triplicate determinations. Representative results of two independent experiments are shown. (C) Splenocytes from SH2-B$^{-/-}$ mice or wild-type littermates were stimulated with 10 μg of anti-CD3ε/ml and cultured for 48 h. Supernatants were collected, and IL-2 or IL-4 in the supernatants was measured by ELISA. The results are presented as the average of duplicate assays.

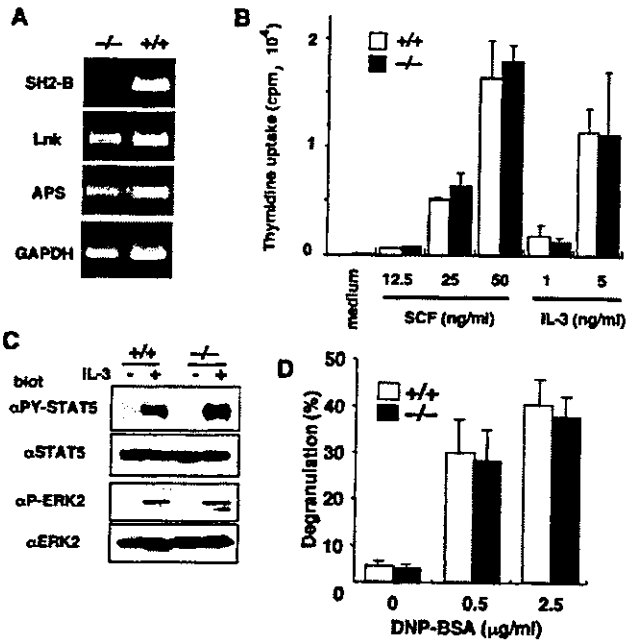

FIG. 4. Normal mast cell function in the absence of SH2-B. (A) RT-PCR analysis for the expression of SH2-B, Lnk, APS, and glyceraldehyde-3-phosphate dehydrogenase (GAPDH). Total RNA from 10^6 BMMCs was used as a template. (B) Proliferation of mast cells induced by IL-3 or SCF. BMMCs obtained from SH2-B$^{-/-}$ mice or wild-type littermates were stimulated with the indicated concentrations of IL-3 or SCF, and proliferation was measured on day 3 by [^{3}H]thymidine incorporation. The values are the mean counts per minute $\times 10^{-3}$ ($\pm$ standard deviation) of triplicate determinations. Representative results of two independent experiments are shown. (C) STAT5 and ERK2 activation in response to IL-3. BMMCs (10^6) were stimulated with 5 ng of IL-3/ml for 20 min, and then cell extracts were immunoblotted with the indicated antibodies. (D) Degranulation of mast cells induced by Fcε-RI cross-linking. BMMCs were sensitized with anti-DNP IgE and then stimulated with the indicated amount of DNP-BSA. The release of β-hexosaminidase was measured as described in Materials and Methods. Percentages of degranulation were calculated by dividing the released β-hexosaminidase by the total β-hexosaminidase stored in cells. Representative results of three independent experiments are shown.

are both expressed in stromal cells in the ovary (data not shown).

IVF experiments show reduced sperm and egg activity. To investigate possible defects in the germ cells of SH2-B-null mice, we conducted IVF experiments. Oocytes collected from SH2-B$^{-/-}$ and wild-type females were inseminated with sperm from wild-type males. As shown in Table 2, 84% of wild-type oocytes had developed to the two-cell stage just 24 h after insemination. When sperm collected from SH2-B$^{-/-}$ mice was used to inseminate wild-type oocytes, a much lower percentage of zygotes developed (15% of that with +/+ × +/+). SH2-B-null oocytes were also significantly impaired in development: only 13 or 10% of SH2-B$^{-/-}$ oocytes developed to the two-cell stage when SH2-B$^{-/-}$ oocytes were inseminated with wild-type or SH2-B$^{-/-}$ sperm, respectively. These observations suggest that both male and female germ cells were defective in fertilization.

Next, to examine sperm-egg fusion, we performed a partial zona dissection on SH2-B$^{-/-}$ eggs followed by insemination with wild-type sperm, or a partial zona dissection on wild-type eggs followed by insemination with SH2B$^{-/-}$ sperm. These procedures did not increase the efficiency of fertilization (data not shown), thereby suggesting that the lower fertilization efficiency of SH2-B$^{-/-}$ egg and sperm is not due to a defect of egg-sperm fusion but rather to the lower activity of the sperm and to immaturity of the eggs.

To determine whether the impaired fertility was due to a defect in germ cells, we did a transplantation experiment. Two-cell-stage zygotes developed by IVF were transplanted into the ampullae of oviducts of female ICR mice, and the number of offspring was counted. Although offspring were obtained with all combinations (Table 2), offspring from the mutant egg-mutant sperm combination were much fewer than from the

TABLE 1. Antibody production in SH2-B$^{-/-}$ mice

Expt and genotype (n)	Antibody response					
	IgM	IgG3	IgG1	IgG2a	IgG2b	IgA
Serum immunoglobulin[a]						
+/+ (7)	140 ± 36	130 ± 50	480 ± 130	620 ± 380	360 ± 110	120 ± 20
−/− (7)	150 ± 39	86 ± 18	280 ± 64	210 ± 61	260 ± 80	69 ± 6.0
Thymus-independent antigen[b,d]						
+/+ (7)	14 ± 3.6					
−/− (5)	13 ± 3.3					
Thymus-dependent antigen[c,d]						
+/+ (5)	12 ± 2.9	2.8 ± 0.49	17 ± 7.0	4.9 ± 0.96	10 ± 4.9	2.0 ± 0.51
−/− (4)	8.4 ± 2.3	3.1 ± 1.8	17 ± 6.3	9.2 ± 4.1	16 ± 11	2.2 ± 0.81

[a] Concentrations (mg/ml) of immunoglobulin subclasses in serum were determined by isotype-specific ELISA.
[b] Antibody response to thymus-independent antigen, TNP-Ficoll. Mice were injected with TNP-Ficoll and the amounts of hapten-specific IgM antibodies were measured by ELISA.
[c] Response to thymus-dependent antigen, BSA. Mice were immunized with BSA and BSA-specific immunoglobulin subclasses were measured. Data shown are the mean ± standard error of the mean for the indicated groups of mice.
[d] Results are expressed as relative titer (10^{-2}).

wild-type–wild-type combination. These results suggest that impaired fertility and the reduced number of offspring of SH2-B-null mice may be caused by a defect in the initial development of fertilized eggs.

Oocytes from SH2-B-null mice have a reduced response to FSH and IGF-I. We examined the response of SH2-B-null female mice to reproductive hormones. Serum hormone levels did not differ between wild-type and SH2-B KO mice (Table 3). Gonadotropin (FSH plus luteinizing hormone [LH]) treatment of wild-type and heterozygous mice resulted in the development of many preantral follicles into antral follicles, while in SH2-B$^{-/-}$ female mice this development was impaired (Fig. 7A). There was a significant decrease in the number of ovulated oocytes in mutant mice, even following treatment to induce superovulation (Fig. 7B). These data indicate that the SH2-B-deficient ovary reduced the response to exogenous gonadotropin stimulation.

To examine function in the microenvironment of the ovary, we did in vitro experiments on COC expansion. Exposure to FSH leads to drastic changes in cumulus cells because of the hyaluronidase sensitivity of the cumulus oophori (Fig. 8A and B). These experiments showed that in wild-type COCs, FSH caused ovarian follicles to expand. In contrast, SH2-B$^{-/-}$ COCs did not expand in 1 μg of FSH/ml (Fig. 8E). We also observed reduced FSH-R mRNA levels in SH2B$^{-/-}$ COC cells (Fig. 8G). Since FSH-R levels have been shown to be regulated by IGF-I, we examined the effect of IGF-I on COC expansion. IGF-I pretreatment did not increase FSH sensitivity of SH2-B$^{-/-}$ COCs (Fig. 8F), which suggested that COCs from SH2-B$^{-/-}$ mice could not respond to IGF-I. FSH stimulates steroid

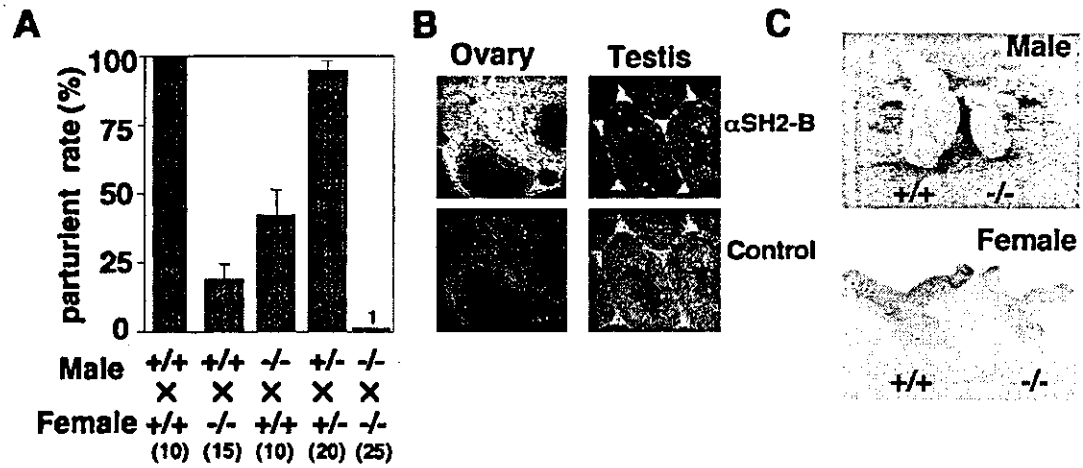

FIG. 5. Reduced fertility and hypoplasia of gonadal tissues in SH2-B$^{-/-}$ mice. (A) Parturition rate of wild-type, SH2-B$^{+/-}$, and SH2-B$^{-/-}$ females and males was examined by caging one male with one or two females with various SH2-B genotypes. The average parturition rate (± standard error of the mean) is shown. The numbers in parentheses indicate the numbers of mating pairs. (B) Localization of SH2-B in wild-type testis and ovary. Immunofluorescence staining was carried out on 5-μm sections with anti-mouse SH2-B polyclonal antibody. Magnification, ×40. (C) Hypoplasia of SH2-B$^{-/-}$ female and male gonads in contrast to those from wild-type mice. Testes were from the wild-type and SH2-B$^{-/-}$ littermates at 73 days after birth. Ovaries were from wild-type and SH2-B$^{-/-}$ littermates at 83 days after birth.

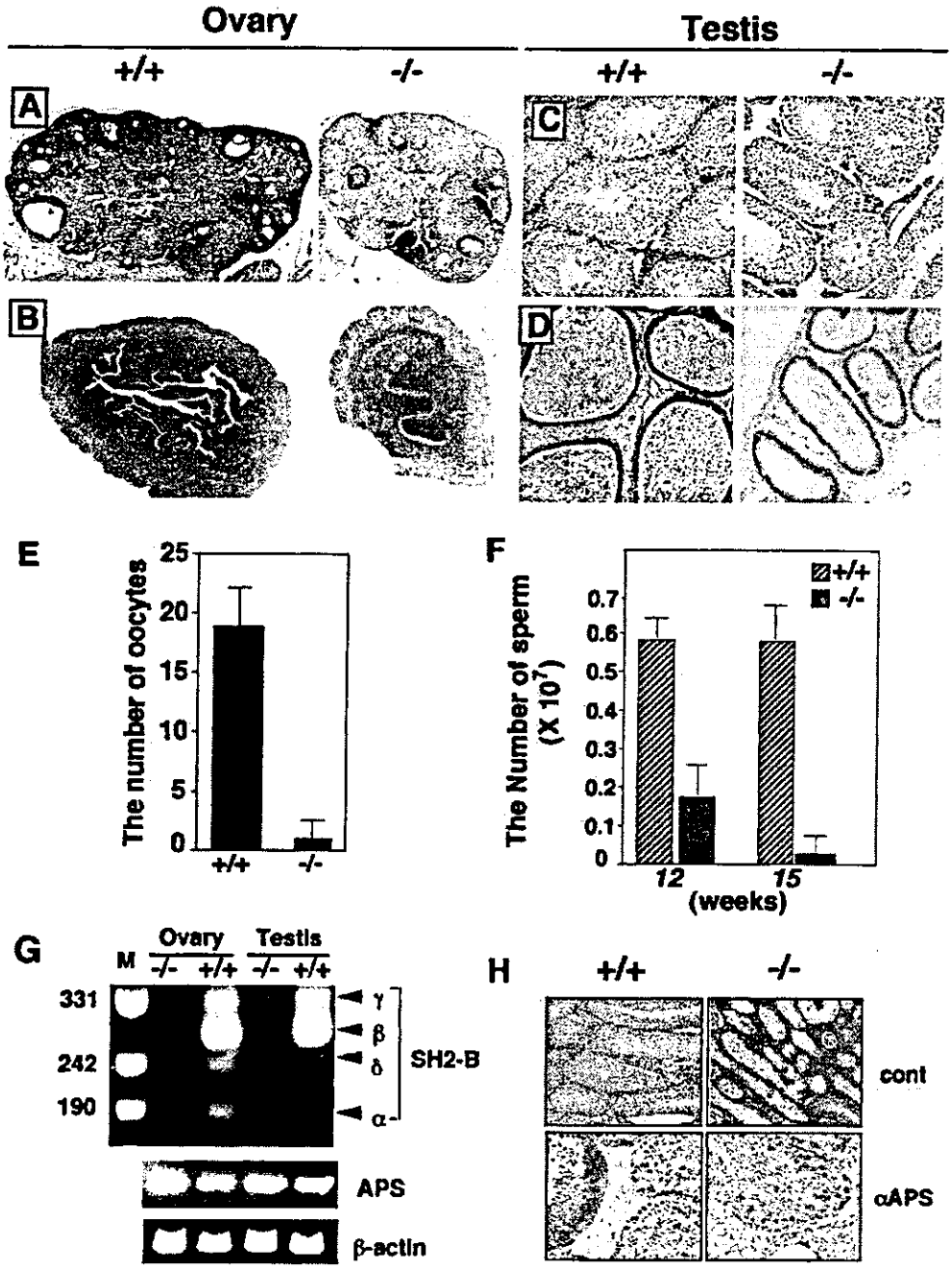

FIG. 6. Dysfunction of gonads of SH2-B-deficient mice. Histological analysis of ovary (A), uterus (B), testis (C), and epididymis (D) from wild-type (+/+) and SH2-B KO (−/−) mice. All sections were fixed overnight in 10% buffered formalin, dehydrated with ethanol, and then embedded in paraffin. Five-micrometer sections stained with hematoxylin and eosin are shown. Magnification, ×50. (E) Number of naturally ovulated oocytes from wild-type and SH2-B-deficient mice. The values are the mean ± standard deviation of triplicate determinations. Mice in estrous were used. (F) Analysis of sperm number from SH2-B-deficient and wild-type male mice. Sperm were collected from the epididymis, suspended in R18S3 medium, and then diluted with PBS. The sperm number is shown as the mean ± standard error of the mean (n = 4). (G) Expression of SH2-B splice variants and APS. After RT of mRNA from ovary and testis of wild-type (+/+) and SH2-B$^{-/-}$ mice, PCR was carried out with specific diagnostic primers (46) to amplify variant-specific fragments of carboxyl-terminal coding regions (indicated on the right) and in parallel to amplify APS and a control β-actin fragment. Products were compared on an ethidium bromide-stained agarose gel with specific size markers (in base pairs) shown on the left. (H) APS expression detected by immunohistochemistry. Testes of wild-type (+/+) and SH2-B KO (−/−) mice were stained with preimmune rabbit IgG (control) or affinity-purified anti-murine APS antibody. Magnification, ×40 (control) and ×100 (αAPS).

TABLE 2. Results of IVF and embryonic transfer[a]

Genotypes		Total no. of oocytes	No. (%) of two-cell-stage embryos	No. of transplanted embryos	No. of offspring
Sperm	Oocyte				
+/+	+/+	83	70 (81.4)	65	28
−/−	+/+	66	10 (15.2)	10	3
+/+	−/−	71	9 (12.6)	9	2
−/−	−/−	77	8 (10.3)	8	1

[a] Sperm from the epididymides were incubated with oocytes treated with hyaluronidase. After 24 h, these inseminated eggs were beginning cleavage, and the number of two-cell eggs was counted. Then, these two-cell-stage embryos were transplanted into ICR mice and the number of offspring was scored.

synthesis in granulosa cells, thereby promoting maturation of oocytes in a paracrine fashion. Since SH2-B is highly expressed in supporting cells (Fig. 5B), these results suggest that dysfunction of supporting cells, probably an IGF-I insensitivity, contributes to the reduced maturation of SH2-B$^{-/-}$ oocytes.

To examine the effect of SH2-B in IGF-I signal transduction, tyrosine phosphorylation of cellular proteins as well as ERK2 MAP activation in COCs were examined in response to IGF-I stimulation (Fig. 8H). A similar phosphorylation of cellular proteins and ERK2 was observed in wild-type and SH2-B$^{-/-}$ mice COCs. This suggests that SH2-B is involved in a signal transduction pathway which is different from the classical MAP kinase pathway.

DISCUSSION

SH2-B function in gonad development. In the present work, we demonstrated that SH2-B is essential for the normal development of gonadal tissues in both male and female mice. IGF-I and FSH signaling has been shown to be essential for spermatogenesis and maintenance of normal sperm production in males (6, 24), and in females it is thought to tightly regulate follicle and oocyte maturation (2, 3, 15, 47). As shown in Fig. 8G, FSH-R levels decreased in SH2-B$^{-/-}$ ovaries and isolated COCs did not respond to IGF-I. The phenotype of SH2-B-null mice partially resembles that of IGF-I-, FSH-, and FSH-R-null mice. Although female FSH-null mice are infertile, males are fertile despite a significant reduction in testis size; the same is true of FSH-R-null mice (1, 11, 24). Based on in vitro analyses, SH2-B was proposed to be a signal-transducing adaptor molecule located downstream of GH, insulin, IGF-I, hepatocyte growth factor, PDGF, and fibroblast growth factor. Of these hormones, IGF-I is thought to be tightly involved in maintaining gonadal function (2, 3, 6). Therefore, the primary defect of the SH2-B$^{-/-}$ mice is probably impaired signaling of IGF-I in gonadal tissues.

In FSH-R-null males, no differences in the levels of FSH and LH were found in the pituitary, even though levels of these

TABLE 3. Serum hormone levels[a]

Genotype	Testosterone	Estradiol	FSH	LH	IGF-I
+/+	1.4 ± 0.7	10.6 ± 2.7	4.0 ± 3.4	1.6 ± 1.1	234 ± 16
−/−	2.6 ± 3.0	11.5 ± 3.2	6.1 ± 3.6	1.7 ± 0.9	235 ± 10

[a] Serum hormone levels (ng/ml) were measured using radioimmunoassay. Four to six mice were used for each assay.

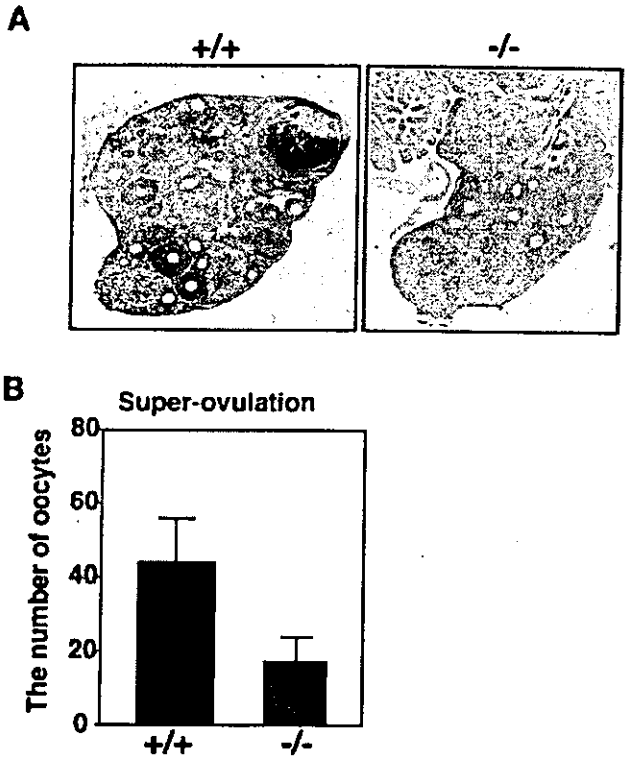

FIG. 7. Comparison of the responsiveness of wild-type and SH2-B-deficient female mice to gonadotropin. (A) Ovaries were treated with gonadotropin to induce superovulation in wild-type and SH2-B-deficient females, fixed with 10% buffered formalin, embedded in paraffin, sectioned at 5 μm, and stained with hematoxylin and eosin. Magnification, ×50. (B) Number of superovulated oocytes. After treatment with PMSG and human chorionic gonadotropin, oocytes were collected from the ampullae of the oviducts of wild-type and SH2-B-deficient mice (n = 5) and the ovulated oocytes were counted.

hormones in serum were elevated. Therefore, it has been suggested that FSH-R-null males are fertile. However, we observed no differences in levels of these hormones in serum in SH2-B-null male and female mice (Table 3). Furthermore, weight and gross morphology of the pituitary gland in SH2-B-null mice were similar to those of wild-type littermates (data not shown), which suggests that dysfunction of the gonads in SH2-B-deficient mice is not due to abnormal function of the pituitary gland. However, one could argue that reduced FSH-R in the ovary should result in an increase in both FSH and LH through negative feedback mechanisms. Similar levels of FSH and LH in SH2-B KO mice to those in wild-type mice could be explained by a small reduction in sex steroid hormone levels in serum. We could not exclude the possibility of dysfunction of the hypothalamus and pituitary, since SH2-B was highly expressed in the brain. Interestingly, insulin receptor substrate 2 (IRS-2) KO mice exhibit similar defects in folliculogenesis, yet LH levels are reduced (7). Therefore, a negative feedback system may be defective in the SH2-B as well as in the IRS-2 KO mice.

IGF-I is produced by various types of cells, and this growth factor has been implicated in a variety of reproductive processes. Leydig and Sertoli cells in males and granulosa and cumulus cells in females carry the IGF-I receptor (15–17, 28).

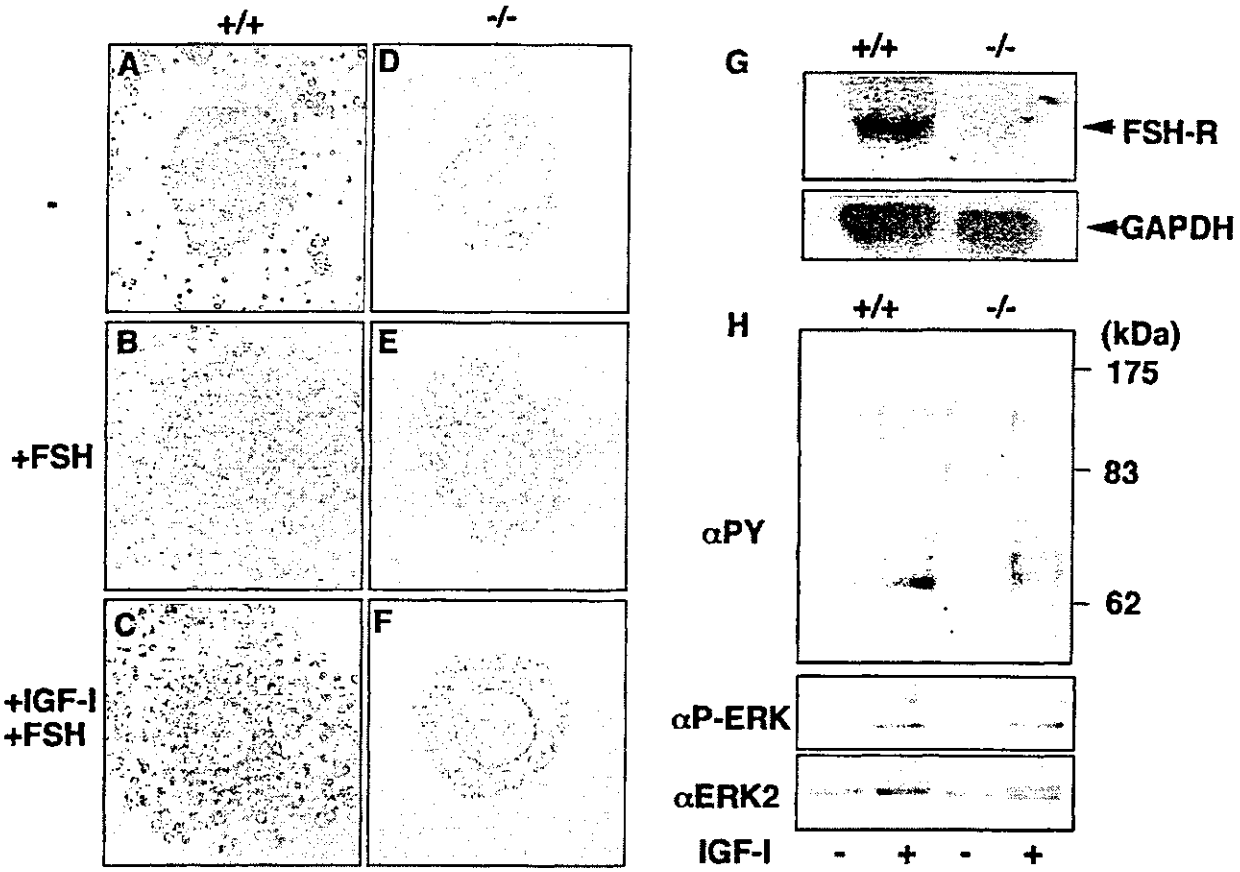

FIG. 8. SH2-B is essential for developing cumulus oophori. A COC expansion assay was performed with wild-type (A, B, and C) and SH2-B-deficient (D, E, and F) COCs. Forty-eight hours after administration of 5 IU of PMSG, Graafian follicles were punctured with needles and the COCs were removed into control Waymouth's medium. COCs were cultured in Waymouth's medium containing 3 mg of BSA/ml without FCS overnight at 37°C (A and D). Wild-type COCs were expanded with 1 μg of FSH/ml (B and E) in Waymouth's medium. COCs were also cultured in Waymouth's medium containing 10 ng of IGF-I/ml for 4 h, followed by 1 μg of FSH/ml (C and F). Similar results were obtained with up to 100 ng of IGF-I/ml. Magnification, ×100. Representative results of three independent experiments are shown. (G) Expression of FSH-R. Total RNA was extracted from ovaries of wild-type (+/+) and SH2-B-null (−/−) mice and hybridized with FSH-R (upper panel) and control glyceraldehyde-3-phosphate dehydrogenase (GAPDH) cDNA (lower panel). (H) Tyrosine phosphorylation of cellular proteins and ERK2 phosphorylation in COCs in response to IGF-I. COCs were collected from two female mice and stimulated with 100 ng of IGF-I/ml for 20 min. Cell extracts were immunoblotted with antiphosphotyrosine (αPY), anti-phosphorylated ERK (αP-ERK), or anti-ERK2 antibodies.

Ovarian granulosa cells contain IGF-I mRNA, secrete IGF-I in vitro and in vivo, and express the IGF-I receptor. IGF-I stimulates both proliferation and differentiation of granulosa and thecal cells in vitro (6, 9, 17). Moreover, IGF-I has been shown to potentiate FSH-stimulated cyclic AMP production, aromatase activity, and LH receptor expression by granulosa cells. IGF-I-deficient mice show partially similar, but more severe, defects than do SH2-B$^{-/-}$ mice. IGF-I-deficient mice show growth retardation, delayed puberty, and ovarian dysfunction (6, 26). Therefore, SH2-B is likely to be an important, although probably not the only, signaling molecule of the IGF-I receptor. A similar pattern of female infertility, including small anovulatory ovaries with reduced numbers of follicles, was observed in female mice lacking the IRS-2 gene, a component of the insulin and IGF-I signaling cascade (7, 22). Thus, SH2-B and IRS-I could be independently necessary for IGF-I signaling pathways in the ovary.

Although APS is expressed in ovary and testis, there was no strong overexpression of APS in gonadal tissues in SH2-B$^{-/-}$ mice (Fig. 6G and H). Furthermore, we found no defect in reproduction in APS$^{-/-}$ and Lnk$^{-/-}$ mice 39; M. Iseki, S. Takaki, and K. Takatsu, unpublished data). Phenotypes of Lnk KO mice (39, 40) as well as our biochemical analyses (42, 44) suggest that Lnk and APS negatively regulate tyrosine kinase signal transduction, while our present study suggests that SH2-B transmits unknown positive signals from the IGF-I receptor. The reason for such differences in functions of SH2-B and APS or Lnk are not clear at present.

Yousaf et al. (46) reported that all SH2-B isoforms augmented IGF-I- and PDGF-induced mitogenesis, although the most pronounced effect was observed with the γ variant. A high level of expression of SH2-Bγ and -β in gonadal tissues (Fig. 6G) may be responsible for the phenotype of SH2-B KO mice. As shown in Fig. 8H, MAP kinase activation in response to IGF-I in COCs was not affected by SH2-B deficiency, suggesting that other pathways are mediated by SH2-B in these cells. Recently, Diakonova et al. reported that SH2-B directly interacts with Rac (10). SH2-B KO mice will provide a useful

tool to define the signaling pathway in which SH2-B mediates the response to IGF-I.

SH2-B is not necessary for other tyrosine kinase signaling. It has been reported that SH2-B binds to the cytoplasmic phosphotyrosine residue of the insulin receptor (4, 27, 43). SH2-B interacts with insulin receptor activation loop phosphorylation sites and undergoes insulin-stimulated tyrosine phosphorylation in vitro (5, 23). Obesity is associated with infertile conditions such as polycystic ovary syndrome (14, 25). We measured blood glucose concentrations after intraperitoneal injection of 2 g of D-(+)-glucose/kg of body weight, but we observed no differences in blood glucose concentrations compared to that in wild-type control mice. These results suggest that SH2-B may not be involved in blood glucose homeostasis in vivo (data not shown). However, IRS-2-null male mice had increased blood glucose concentrations compared to wild-type controls (7). Moreover, in IRS-2 KO mice the plasma concentrations of LH, prolactin, and sex steroids were low, but this was not the case in SH2-B KO mice. This is probably because the expression of SH2-B is restricted to tissues surrounding germ cells in gonadal organs and SH2-B is not directly involved in the function of the germ cells and pituitary gland.

The anterior pituitary gland plays an important role in regulating the normal reproductive status in mammals. However, the size, gross anatomy, and histology of the pituitary gland of SH2-B-null mice is normal (data not shown). These observations support the idea that the cause of the impaired fertility in SH2-B$^{-/-}$ mice is in the cells surrounding the germ cells, rather than in the germ cells themselves.

Both APS and SH2-B have been shown to be involved in the NGF-induced Ras-MAP kinase signaling cascade. A dominant negative mutant of SH2-Bβ when overexpressed in PC12 cells acts to block NGF-induced neurite outgrowth (12). Thus, SH2-B may be downstream of the Trk tyrosine kinase. Consistent with this finding, SH2-B is highly expressed in the brain. However, when we conducted an in vitro NGF-induced neurite outgrowth assay with dorsal root ganglion cells from SH2-B-null mice, we observed no differences in NGF sensitivity of the dorsal root ganglion cells (data not shown). Thus, either SH2-B is not a major player in NGF signaling or APS can compensate for SH2-B function in SH2-B-null mice.

SH2-Bβ has been reported to be involved in the JAK2 signaling activated by GH (8, 18, 35). Importantly, SH2-Bβ potentiates JAK2 kinase activity (31, 32). Partial growth retardation of SH2-B$^{-/-}$ mice suggests some impairment of GH signaling. However, we obtained no evidence that SH2-B is a JAK2 activator. For example, when stimulated by IL-3, the response of mast cells from SH2-B$^{-/-}$ mice was similar to that of wild-type mice (Fig. 4). We also observed that GH-induced JAK2/STAT5 activation as well as IGF-I induction occurred normally in SH2-B-null mouse liver (data not shown). Thus, SH2-B may be dispensable or unnecessary for JAK2 activity. Further study is necessary to define the role of SH2-B in the GH/JAK2 pathway.

ACKNOWLEDGMENTS

We thank H. Ohgusu and Y. Kawabata for technical assistance, M. Kojima, M. Kamei, Y. Komatsu, and M. Okabe for critical discussion and comments, and M. Ohara for language assistance.

This work was supported by Grants-in-Aid (for Y.A.) and Special Coordination Funds (for T.K.) from the Ministry of Education, Science, Technology, Sports and Culture of Japan, the Japan Health Science Foundation, the Human Frontier Science Program, Mochida Memorial Foundation, and the Japan Research Foundation for Clinical Pharmacology. S.O. is supported by a fellowship from the Japan Society for the Promotion of Science.

REFERENCES

1. **Abel, M. H., A. N. Wootton, V. Wilkins, I. Huhtaniemi, P. G. Knight, and H. M. Charlton.** 2000. The effect of a null mutation in the follicle-stimulating hormone receptor gene on mouse reproduction. Endocrinology **141**:1795–1803.
2. **Adashi, E. Y., C. E. Resnick, and R. G. Rosenfeld.** 1990. Insulin-like growth factor-I (IGF-I) and IGF-II hormonal action in cultured rat granulosa cells: mediation via type I but not type II IGF receptors. Endocrinology **126**:216–222.
3. **Adashi, E. Y., C. E. Resnick, A. J. D'Ercole, M. E. Svoboda, and J. J. Van Wyk.** 1985. Insulin-like growth factors as intraovarian regulators of granulosa cell growth and function. Endocr. Rev. **6**:400–420.
4. **Ahmed, Z., and T. S. Pillay.** 2001. Functional effects of APS and SH2-B on insulin receptor signalling. Biochem. Soc. Trans. **29**:529–534.
5. **Ahmed, Z., B. J. Smith, K. Kotani, P. Wilden, and T. S. Pillay.** 1999. APS, an adapter protein with a PH and SH2 domain, is a substrate for the insulin receptor kinase. Biochem. J. **341**:665–668.
6. **Baker, J., M. P. Hardy, J. Zhou, C. Bondy, F. Lupu, A. R. Bellve, and A. Efstratiadis.** 1996. Effects of an Igf1 gene null mutation on mouse reproduction. Mol. Endocrinol. **10**:903–918.
7. **Burks, D. J., J. F. de Mora, M. Schubert, D. J. Withers, M. G. Myers, H. H. Towery, S. L. Altamuro, C. L. Flint, and M. F. White.** 2000. IRS-2 pathways integrate female reproduction and energy homeostasis. Nature **407**:377–382.
8. **Carter-Su, C., L. Rui, and M. R. Stofega.** 2000. SH2-B and SIRP: JAK2 binding proteins that modulate the actions of growth hormone. Recent Prog. Horm. Res. **55**:293–311.
9. **Davoren, J. B., B. G. Kasson, C. H. Li, and A. J. Hsueh.** 1986. Specific insulin-like growth factor (IGF) I- and II-binding sites on rat granulosa cells: relation to IGF action. Endocrinology **119**:2155–2162.
10. **Diakonova, M., D. R. Gunter, J. Herrington, and C. Carter-Su.** SH2-Bβ is a Rac binding protein that regulates cell motility. J. Biol. Chem., in press.
11. **Dierich, A., M. R. Sairam, L. Monaco, G. M. Fimia, A. Gansmuller, M. LeMeur, and P. Sassone-Corsi.** 1998. Impairing follicle-stimulating hormone (FSH) signaling in vivo: targeted disruption of the FSH receptor leads to aberrant gametogenesis and hormonal imbalance. Proc. Natl. Acad. Sci. USA **95**:13612–13617.
12. **Eggert, A., N. Ikegaki, X. Liu, T. T. Chou, V. M. Lee, J. Q. Trojanowski, and G. M. Brodeur.** 2000. Molecular dissection of TrkA signal transduction pathways mediating differentiation in human neuroblastoma cells. Oncogene **19**:2043–2051.
13. **Eppig, J. J.** 1979. Gonadotropin stimulation of the expansion of cumulus oophori isolated from mice: general conditions for expansion in vitro. J. Exp. Zool. **208**:111–120.
14. **Franks, S., C. Gilling-Smith, H. Watson, and D. Willis.** 1999. Insulin action in the normal and polycystic ovary. Endocrinol. Metab. Clin. North Am. **28**:361–378.
15. **Hammond, J. M., J. L. Baranao, D. Skaleris, A. B. Knight, J. A. Romanus, and M. M. Rechler.** 1985. Production of insulin-like growth factors by ovarian granulosa cells. Endocrinology **117**:2553–2555.
16. **Hernandez, E. R., A. Hurwitz, A. Vera, A. Pellicer, E. Y. Adashi, D. LeRoith, Jr., and C. T. Roberts.** 1992. Expression of the genes encoding the insulin-like growth factors and their receptors in the human ovary. J. Clin. Endocrinol. Metab. **74**:419–425.
17. **Hernandez, E. R., Jr., C. T. Roberts, D. LeRoith, and E. Y. Adashi.** 1989. Rat ovarian insulin-like growth factor I (IGF-I) gene expression is granulosa cell-selective: 5′-untranslated mRNA variant representation and hormonal regulation. Endocrinology **125**:572–574.
18. **Herrington, J., M. Diakonova, L. Rui, D. R. Gunter, and C. Carter-Su.** 2000. SH2-B is required for growth hormone-induced actin reorganization. J. Biol. Chem. **275**:13126–13133.
19. **Hogan, B., R. Beddington, F. Constantini, and E. Lacy.** 1994. Manipulating the mouse embryo, a laboratory manual, 2nd ed. Cold Spring Harbor Laboratory Press, New York, N.Y.
20. **Huang, X., Y. Li, K. Tanaka, K. G. Moore, and J. I. Hayashi.** 1995. Cloning and characterization of Lnk, a signal transduction protein that links T-cell receptor activation signal to phospholipase C gamma 1, Grb2, and phosphatidylinositol 3-kinase. Proc. Natl. Acad. Sci. USA **92**:11618–11622.
21. **Iseki, M., S. Takaki, and K. Takatsu.** 2000. Molecular cloning of the mouse APS as a member of the Lnk family adaptor proteins. Biochem. Biophys. Res. Commun. **272**:45–54.
22. **Joshi, R. L., B. Lamothe, N. Cordonnier, K. Mesbah, E. Monthioux, J. Jami, and D. Bucchini.** 1996. Targeted disruption of the insulin receptor gene in the mouse results in neonatal lethality. EMBO J. **15**:1542–1547.
23. **Kotani, K., P. Wilden, and T. S. Pillay.** 1998. SH2-Bα is an insulin-receptor

adapter protein and substrate that interacts with the activation loop of the insulin-receptor kinase. Biochem. J. 335:103–109.
24. **Kumar, T. R., Y. Wang, N. Lu, and M. M. Matzuk.** 1997. Follicle stimulating hormone is required for ovarian follicle maturation but not male fertility. Nat. Genet. 15:201–204.
25. **Legro, R. S., R. Spielman, M. Urbanek, D. Driscoll III, J. F. Strauss, and A. Dunaif.** 1998. Phenotype and genotype in polycystic ovary syndrome. Recent Prog. Horm. Res. 53:217–256.
26. **Liu, J. P., J. Baker, A. S. Perkins, E. J. Robertson, and A. Efstratiadis.** 1993. Mice carrying null mutations of the genes encoding insulin-like growth factor I (Igf-1) and type 1 IGF receptor (Igf1r). Cell 75:59–72.
27. **Nelms, K., T. J. O'Neill, S. Li, S. R. Hubbard, T. A. Gustafson, and W. E. Paul.** 1999. Alternative splicing, gene localization, and binding of SH2-B to the insulin receptor kinase domain. Mamm. Genome 10:1160–1167.
28. **Oliver, J. E., T. J. Aitman, J. F. Powell, C. A. Wilson, and R. N. Clayton.** 1989. Insulin-like growth factor I gene expression in the rat ovary is confined to the granulosa cells of developing follicles. Endocrinology 124:2671–2679.
29. **Osborne, M. A., S. Dalton, and J. P. Kochan.** 1995. The yeast trihybrid system—genetic detection of trans-phosphorylated ITAM-SH2-interactions. Bio/Technology 13:1474–1478.
30. **Parganas, E., D. Wang, D. Stravopodis, D. J. Topham, J. C. Marine, S. Teglund, E. F. Vanin, S. Bodner, O. R. Colamonici, J. M. van Deursen, G. Grosveld, and J. N. Ihle.** 1998. Jak2 is essential for signaling through a variety of cytokine receptors. Cell 93:385–395.
31. **Qian, X., A. Riccio, Y. Zhang, and D. D. Ginty.** 1998. Identification and characterization of novel substrates of Trk receptors in developing neurons. Neuron 21:1017–1029.
32. **Riedel, H., J. Wang, H. Hansen, and N. Yousaf.** 1997. PSM, an insulin-dependent, pro-rich, PH, SH2 domain containing partner of the insulin receptor. J. Biochem. (Tokyo) 122:1105–1113.
33. **Rui, L., and C. Carter-Su.** 1998. Platelet-derived growth factor (PDGF) stimulates the association of SH2-Bβ with PDGF receptor and phosphorylation of SH2-Bβ. J. Biol. Chem. 273:21239–21245.
34. **Rui, L., and C. Carter-Su.** 1999. Identification of SH2-Bβ as a potent cytoplasmic activator of the tyrosine kinase Janus kinase 2. Proc. Natl. Acad. Sci. USA 96:7172–7177.
35. **Rui, L., D. R. Gunter, J. Herrington, and C. Carter-Su.** 2000. Differential binding to and regulation of JAK2 by the SH2 domain and N-terminal region of SH2-Bβ. Mol. Cell. Biol. 20:3168–3177.
36. **Rui, L., J. Herrington, and C. Carter-Su.** 1999. SH2-B, a membrane-associated adapter, is phosphorylated on multiple serines/threonines in response to nerve growth factor by kinases within the MEK/ERK cascade. J. Biol. Chem. 274:26485–26492.
37. **Rui, L., L. S. Mathews, K. Hotta, T. A. Gustafson, and C. Carter-Su.** 1997. Identification of SH2-Bβ as a substrate of the tyrosine kinase JAK2 involved in growth hormone signaling. Mol. Cell. Biol. 17:6633–6644.
38. **Takaki, S., J. D. Watts, K. A. Forbush, N. T. Nguyen, J. Hayashi, J. Alberola-Ila, R. Aebersold, and R. M. Perlmutter.** 1997. Characterization of Lnk, an adaptor protein expressed in lymphocytes. J. Biol. Chem. 272:14562–14570.
39. **Takaki, S., K. Sauer, B. M. Iritani, S. Chien, Y. Ebihara, K. Tsuji, K. Takatsu, and R. M. Perlmutter.** 2000. Control of B cell production by the adaptor protein Lnk. Definition of a conserved family of signal-modulating proteins. Immunity 13:599–609.
40. **Takaki, S., H. Morita, Y. Tezuka, and K. Takatsu.** 2002. Enhanced hematopoiesis by hematopoietic progenitor cells lacking intracellular adaptor protein, Lnk. J. Exp. Med. 195:151–161.
41. **Uehara, S., Y. Hitoshi, F. Numata, M. Makino, M. Howard, T. Mizuochi, and K. Takatsu.** 1994. An IFN-gamma-dependent pathway plays a critical role in the pathogenesis of murine immunodeficiency syndrome induced by LP-BM5 murine leukemia virus. Int. Immunol. 6:1937–1947.
42. **Wakioka, T., A. Sasaki, K. Mitsui, M. Yokouchi, A. Inoue, S. Komiya, and A. Yoshimura.** 1999. APS, an adaptor protein containing PH and SH2 domains inhibits the JAK-STAT pathway in collaboration with c-Cbl. Leukemia 13: 760–767.
43. **Wang, J., and H. Riedel.** 1998. Insulin-like growth factor-I receptor and insulin receptor association with a Src homology-2 domain-containing putative adapter. J. Biol. Chem. 273:3136–3139.
43a. **World Health Organization.** 1992. WHO laboratory manual for the examination of human semen and sperm-cervical mucus interaction. Cambridge University Press, Cambridge, England.
44. **Yokouchi, M., R. Suzuki, M. Masuhara, S. Komiya, A. Inoue, and A. Yoshimura.** 1997. Cloning and characterization of APS, an adaptor molecule containing PH and SH2 domains that is tyrosine phosphorylated upon B-cell receptor stimulation. Oncogene 15:7–15.
45. **Yokouchi, M., T. Wakioka, H. Sakamoto, H. Yasukawa, S. Ohtsuka, A. Sasaki, M. Ohtsubo, M. Valius, A. Inoue, S. Komiya, and A. Yoshimura.** 1999. APS, an adaptor protein containing PH and SH2 domains, is associated with the PDGF receptor and c-Cbl, and inhibits PDGF-induced mitogenesis. Oncogene 18:759–768.
46. **Yousaf, N., Y. Deng, Y. Kang, and H. Riedel.** 2001. Four PSM/SH2-B alternative splice variants and their differential roles in mitogenesis. J. Biol. Chem. 276:40940–40948.
47. **Zhou, J., T. R. Kumar, M. M. Matzuk, and C. Bondy.** 1997. Insulin-like growth factor I regulates gonadotropin responsiveness in the murine ovary. Mol. Endocrinol. 11:1924–1933.

International Immunology, Vol. 14, No. 9, pp. 1055–1064

NF-κB is required for CD38-mediated induction of $C_\gamma 1$ germline transcripts in murine B lymphocytes

Hiroaki Kaku[1], Keisuke Horikawa[1], Yuichi Obata[2], Ichiro Kato[3], Hiroshi Okamoto[3], Nobuo Sakaguchi[4], Steve Gerondakis[5] and Kiyoshi Takatsu[1]

[1]Division of Immunology, Department of Microbiology and Immunology, Institute of Medical Science, University of Tokyo, Tokyo 108-8639, Japan
[2]Department of Pathology, Aichi Cancer Center, Nagoya 464-8681, Japan
[3]Department of Biochemistry, Tohoku University Graduate School of Medicine, Sendai 980-8575, Japan
[4]Department of Immunology, Kumamoto University School of Medicine, Kumamoto 960-8575, Japan
[5]Walter and Eliza Hall Institute of Medical Research, Royal Melbourne Hospital, Victoria 3050, Australia

Keywords: Bruton's tyrosine kinase, c-Rel, IgH switch recombination, IL-5, phosphatidylinositol-3 kinase, transcription factors

Abstract

Ligation of CD38 on murine B cells with agonistic anti-CD38 mAb induces B cell proliferation, expression of germline γ1 transcripts and enhances IL-5 receptor expression. This leads to Ig class switch recombination from the μ to γ1 heavy chain gene, and high levels of IgM and IgG1 production, particularly in response to anti-CD38 and IL-5 co-stimulation. Although some of the post-receptor signaling events initiated by CD38 ligation have been characterized, signaling pathways involved in CD38-mediated germline γ1 transcript expression in B cells are poorly understood. Here we show that CD38 ligation of murine splenic B cells activates members of the NF-κB/Rel family of proteins including c-Rel, p65 and p50. The activation patterns and kinetics of NF-κB-like proteins in CD38-stimulated B cells differ somewhat from those seen in CD40-stimulated B cells. Activation of NF-κB-like proteins by CD38 ligation is not observed in splenic B cells from Bruton's tyrosine kinase (Btk)-deficient ($Btk^{-/-}$) mice, with inhibitors of protein kinase C (PKC) and phosphatidylinositol (PI)-3 kinase also suppressing NF-κB activation in CD38-activated B cells. We infer from these results that activation of Btk, PI-3 kinase and PKC play, at least in part, important roles in the induction of NF-κB in CD38-stimulated murine B cells. Consistent with a role for NF-κB/Rel signaling in CD38-mediated germline γ1 transcript expression, $p50^{-/-}$ B cells show significant impairment of germline γ1 transcript expression in response to CD38 ligation, whereas the CD40-induced response was not altered. In contrast, $c\text{-}Rel^{-/-}$ B cells show a severe impairment of germline γ1 transcript expression in response to CD38 or CD40 ligation. These results indicate an essential role for NF-κB proteins in the induction of germline γ1 transcripts by CD38-ligated murine B cells giving rise to IL-5-induced IgG1 production.

Introduction

The NF-κB/Rel family of transcription factors, which includes p50, p52, p65 (RelA), RelB and c-Rel, forms homodimers and heterodimers that in most cell types are retained as inactive complexes in the cytoplasm by specific inhibitor (IκB) proteins (1–7). Cellular activation by a range of stimuli involved in inflammation and immunity, such as BCR cross-linkers, CD40 ligand, cytokines, chemokines and lipopolysaccharide (LPS), leads to the phosphorylation and degradation of the IκB component of the NF-κB complex, resulting in the translocation of NF-κB/Rel complexes to the nucleus (1,2,5,6). Subsequent binding of NF-κB to decameric κB sequence motifs within the promoter/enhancer of a wide variety of genes plays a key role in regulating their transcription in a positive manner (8). The subunits of the NF-κB/Rel family of transcrip-

The first two authors contributed equally to this work

Correspondence to: K. Takatsu; E-mail: takatsuk@ims.u-tokyo.ac.jp

Transmitting editor: K. Sugamura

Received 19 April 2002, *accepted* 12 June 2002

tion factors can interact with each other to create different heterodimeric forms with resulting differences in binding specificity, function and interactions with other transcription factors. Pre-B cells express mainly p50 and p65, whereas p50 and c-Rel predominate in mature B cells.

BCR cross-linking leads to the activation of Syk, phosphatidylinositol (PI)-3 kinase, Bruton's tyrosine kinase (Btk), BLNK, phospholipase C (PLC)-γ2, protein kinase C (PKC) and NF-κB (9). Btk acts in concert with Syk to phosphorylate and activate PLC-γ2 (10,11), which in turn mediates production of the second messengers inositol 1,4,5-triphosphate and diacylglycerol (12). These second messengers stimulate the activity of PKC and increase intracellular calcium levels, resulting the activation of downstream transcription factors (13,14). It has recently been shown that Btk (15,16), BLNK (17), PLC-γ2 (18) and PKC (19,20) are all involved in BCR-induced NF-κB activation. In addition, PI-3 kinase gene-targeted ($p85^{-/-}$) mice reveal a profoundly impaired B cell phenotype (21,22). Whilst PI-3 kinase promotes cell survival by activating Akt kinase, which phosphorylates and inactivates the pro-apoptotic molecule, Bad (23), a connection between Akt and IKK-γ has also been shown to be responsible for targeting IκB for degradation and NF-κB activation (24,25).

CD38 is a type II transmembrane glycoprotein that possesses both ADP-ribosyl cyclase and cADP-ribosyl hydrolase activities, and is widely expressed in both hematopoietic and non-hematopoietic cells (26–32). Murine CD38 is expressed in follicular B cells, but is down-regulated in germinal center B cells (30,33,34). Stimulation of $CD38^{+}$ lymphocytes with agonistic anti-CD38 mAb has profound effects on cellular viability, activation, proliferation and differentiation (29,30,35). We previously reported that ligation of splenic B-2 cells with agonistic anti-CD38 (clone CS/2) induces the expression of germline γ1 transcripts, enhances the expression of the IL-5 receptor α chain (IL-5Rα) and prevents B cell apoptosis (35–37). Furthermore, IL-5 stimulation of anti-CD38-activated B-2 cells induces μ–γ1 class switch recombination (CSR) and IgM and IgG1 production in an IL-4-independent manner (37–39). Because of its multiple functions, the signaling pathways triggered by CD38 are expected to be diverse. CD38 ligation by anti-CD38 facilitates activation of tyrosine kinases (Lyn and Btk) (36,41,42), PI-3 kinase (43,44) and phosphorylation of c-Cbl (45). Nonetheless, a direct link between specific signaling pathway and the expression of germline γ1 transcripts remains unclear.

B cells lacking p50 (46–48), c-Rel (46,49,50), RelB (51) and, to a lesser extent, p52 have proliferative defects that may depend upon the manner by which the B cells become activated. The presence of multiple NF-κB/Rel binding sites in the Ig heavy chain locus including I regions and the switch regions has further suggested a potential role for NF-κB/Rel family members in regulating CSR. Interestingly, through studies performed in knockout mice, it became clear that individual members of the NF-κB family have distinct roles in the immune system. Snapper *et al.*, using B cells from p50/NF-κB1-deficient mice, demonstrated that p50/NF-κB plays key selective roles in germline heavy chain RNA expression and CSR (48). They also reported results obtained by using B cells genetically deficient in the c-Rel transactivation domain (Δc-Rel) that Δc-Rel B cells failed to switch to IgG3 in response to LPS alone, or to IgG1 or IgE in response to LPS plus IL-4 (50). These failures of CSR are associated with a corresponding loss of germline γ3, γ1 or ε RNA. The ability of Δc-Rel B cells to switch to IgG1 can be restored through the action(s) of additional stimuli that were associated with induction of normal levels of germline γ1 RNA expression relative to controls (50). Their data demonstrated a key and selective role for c-Rel in the regulation of CSR, and suggested the distinct differences in the Ig isotype induction profiles of B cells lacking c-Rel compared with those deficient in p50/NF-κB.

To gain a better understanding of the role of NF-κB in the cellular activation of CD38-ligated B cells, we analyzed splenic B cells from $p50^{-/-}$ and $c\text{-}Rel^{-/-}$ mice for their ability to undergo proliferation, germline γ1 RNA expression and IgG1 production. We found that both the p50 and c-Rel proteins play an important role in CD38-induced germline γ1 gene expression. We will also discuss the roles of PI-3 kinase, Btk and PKC in the CD38-dependent activation of the NF-κB/Rel family proteins.

Methods

Mice

Female C57BL/6 and BALB/c mice were purchased from Japan SLC (Hamamatsu, Japan) and used at 8–12 weeks of age. $CD38^{-/-}$ mice and $c\text{-}Rel^{-/-}$ and (49,52) were backcrossed to C57BL/6 mice for eight generations and used for experimentation at 8–12 weeks of age. The genotype of $CD38^{-/-}$ mice was determined by PCR of ear DNA using the following primers: C30 (5′-GTCAACCCCCTAGAGTAAGCAGCAA-3′), C63 (5′-CAAGGGTCTACACAGGATCACCAAG-3′) and L129 (5′-TCTCAGGAGGTATCAGTTCAAACCC-3′). The $p50^{-/-}$ mice and wild-type littermates were purchased from the Jackson Laboratory (Bar Harbor, ME). $Btk^{-/-}$ mice (53), kindly provided by Dr Fred Alt (Harvard University, Boston, MA), were backcrossed to C57BL/6 mice for seven generations and maintained in our animal facility. All mice were housed in microisolator cages under pathogen-free conditions, maintained on a diet of laboratory chow and water available *ad libitum* in the animal facility of the Institute of Medical Science, University of Tokyo. All experiments were performed according to the guidelines for animal treatment at the Institute of Medical Science, University of Tokyo.

Antibodies and reagents

Agonistic mAb for murine CD38 (clone CS/2, rat IgG1) and CD40 (clone LB429, rat IgG2a) were prepared as previously described (35,54). Affinity-purified $F(ab')_2$ fragments of goat anti-mouse IgM antibody and LPS were purchased from Cappel (Durham, NC) and Difco (Detroit, MI) respectively. Streptavidin-conjugated magnetic beads were purchased from Miltenyi Biotec (Bergisch Gladbach, Germany). The following mAb were obtained from ATCC (Rockville, MD): RA3-6B2 (anti-B220), 2.4G2 (anti-mouse FcγR) and M1/70 (anti-Mac-1). Anti-mIL-5Rα (clone H7, rat IgG1) was prepared as described (55,56). Purified mAb was coupled with biotin (Pierce, Rockford, IL), FITC (Sigma, St Louis, MO) or phycoerythrin (PE; Pierce). Streptavidin–PE was purchased from Life Technologies (Tokyo, Japan). Mouse IL-4 was purified from cultured supernatant of IL-4-producing cells using 11B11